

SUPPLEMENTAL MATERIAL

Multi-omics of Tissue Extracellular Vesicles Identifies Unique Modulators of Atherosclerosis and Calcific Aortic Valve Stenosis

Blaser MC, et al.

Correspondence to: Elena Aikawa (eaikawa@bwh.harvard.edu)

Supplemental Detailed Methods

Unless otherwise noted, all materials were purchased from Sigma-Aldrich.

Human tissue collection

Diseased human calcified carotid artery atherosclerotic plaques were obtained from patients undergoing surgical carotid endarterectomies indicated due to carotid artery stenosis. Diseased human calcified aortic valve (AV) leaflets were obtained from patients with tricuspid AVs undergoing AV replacement surgeries indicated due to AV stenosis. Surgical donor inclusion criteria included hematocrit >25% and patient age between 20-90 years. Donors with congenital bicuspid AVs were excluded from analysis in this study. Tissue was immediately transferred from the operating room in high-glucose Dulbecco's modified Eagle's medium (DMEM, Gibco 10569010) on ice and was stored at 4°C until further processing within 45 minutes of removal in the operating room prior to freezing at -80°C. Normal carotid arteries and tricuspid AVs destined for isolation of tissue-entrapped extracellular vesicles (EVs) were collected from autopsy donors, transferred, and processed as above with a mean post-mortem interval of 20.6 hours. Only donors who expired due to non-cardiac and non-COVID-19-associated death were

included in this study. Prior to inclusion, normal carotid and AV tissues were also screened to ensure absence of any gross/macrosopic signs of disease including intimal/leaflet thickening, lipid accumulation, fibrosis, or calcification by a trained pathologist. Normal tissue samples destined for whole-tissue global proteomics (Figure S7) were collected from carotid arteries from autopsy and tricuspid AVs from heart transplant recipients due to idiopathic cardiomyopathy, and handled as described above. We do not have IRB approval under 1999P001348 to retroactively collect clinical information from a small subset of the carotid endarterectomy donors.

Composition of (multi-)omics sub-studies

The “**Whole-Tissue Proteomics**” sub-study is presented in Figure 2 (and expanded in Figures S5, S6, S8-S10). It was conducted on 3 stages of disease (paired non-diseased, fibrotic, and calcified regions per donor) dissected from specimens excised by carotid endarterectomy (due to carotid artery stenosis; n=16) and aortic valve replacement (due to aortic valve stenosis; n=18). Proteomics was performed on a Thermo Orbitrap Fusion Lumos mass spectrometer.

The “**Supplemental Whole-Tissue Proteomics**” sub-study is presented in Figure S7. It was conducted on **i)** intact normal specimens (n=3 carotid arteries from autopsy, n=5 aortic valves from heart transplants; no dissection of disease stages/regions), and **ii)** 3 stages of disease (paired non-diseased, fibrotic, and calcified regions per donor) dissected from specimens excised by carotid endarterectomy (due to carotid artery stenosis; n=12) and aortic valve replacement (due to aortic valve stenosis; n=9). The carotid artery stenosis donors and aortic valve stenosis donors included in this analysis are sub-sets of the 16 carotid artery stenosis donors and 18 aortic valve stenosis donors presented in the “Whole-Tissue Proteomics” study. Proteomics was performed on a Thermo Q Exactive Orbitrap mass spectrometer.

The “**EV Isolation Optimization**” sub-study aimed at development and optimization of a method to isolate extracellular vesicles from human cardiovascular tissues is presented in Figure 3 (and expanded in Figures S11-S15). It was conducted on intact specimens (no dissection of disease stages/regions). Specimens were excised by carotid endarterectomy (due to carotid artery stenosis; n=3) and aortic valve replacement (due to aortic valve stenosis; n=4). Proteomics was performed on a Thermo Orbitrap Fusion Lumos mass spectrometer. These donors are a different cohort than those included in the “Whole-Tissue Proteomics” or “Tissue EV Vesiculomics” sub-studies.

The “**Tissue EV Vesiculomics**” sub-study is presented in Figures 4-7 (and expanded in Figures S16-S26). It was conducted on intact specimens (no dissection of disease stages/regions). Normal specimens originated from autopsy (normal carotid arteries [n=6] and normal aortic valves [n=6]), while diseased samples were excised by carotid endarterectomy (due to carotid artery stenosis; n=4) and aortic valve replacement (due to aortic valve stenosis; n=4). Proteomics was performed on a Thermo Orbitrap Fusion Lumos mass spectrometer. These donors are a different cohort than those included in the “Whole-Tissue Proteomics” or “EV Isolation Optimization” sub-studies.

Whole-tissue lysis

For disease stage-specific global proteomics of whole tissues, calcified carotid artery atherosclerotic plaque and calcified aortic valve tissue samples (from carotid endarterectomies and valve replacement surgeries for AV stenosis, respectively) were each separated by disease stage into macroscopically distinct non-diseased, fibrotic, and calcified segments per sample as described previously.^{21,51} Morphologically, non-diseased regions appeared macroscopically

normal, non-thickened, translucent, and pliable with well-defined anatomy. Fibrotic regions were grossly thickened, stiffened, and opaque. Calcified areas had large visible and mineralized nodules that were hardened when probed with forceps. von Kossa staining confirmed calcification, while H&E verified inflammation and fibrosis (Figures S6 and S18). Normal tissue samples (Figure S7) were processed intact. Tissues were pulverized in liquid nitrogen and re-suspended on ice in RIPA buffer (Thermo Scientific Pierce, 89900) with protease inhibitor (Roche, cOmplete ULTRA tablets, 45892970001) and phosphatase inhibitor (Roche, PhosSTOP tablets, 4906845001), and vortexed for 30 seconds.

Extracellular vesicle isolation

Enzymatic digestion

Intact carotid artery (normal from autopsy, diseased atherosclerotic plaques from carotid endarterectomies) and intact aortic valve (normal from autopsy, diseased from valve replacement surgeries for AV stenosis) tissue samples underwent enzymatic digestion largely as described previously.⁵² In brief, intact (non-disease stage-separated) tissue samples were rinsed briefly in sterile phosphate buffered saline without calcium or magnesium (PBS^{-/-}, Corning 46-013-CM), scraped gently on each side with a razor blade to remove the endothelium, and rinsed again. Tissue was then roughly chopped into ~5 mm³ cubes and incubated at 37°C for 1 hour in 1 mg/ml of filter-sterilized collagenase type IA-S from *Clostridium histolyticum* (Sigma-Aldrich C5894) in DMEM, mixing every 20 minutes. After 1 hour, samples were vortexed briefly, the collagenase solution was removed, and tissue pieces were rinsed briefly with DMEM. The collagenase solution and DMEM rinse were pooled, centrifuged at 500xg for 5 minutes, and the resulting supernatant was stored at 4°C. Tissue pieces were then incubated again in 1 mg/ml collagenase for a further 3 hours at 37°C, mixing every 30 minutes. After 3 hours, the digest was vortexed briefly and strained through a 40 µm cell strainer. A

DMEM rinse followed and was again strained at 40 μm . The resultant collagenase solution and DMEM rinse were pooled and centrifuged at 500xg for 5 minutes. The resultant 3-hour supernatant was pooled with the 1-hour supernatant and stored at -80°C . The 500xg pellet was resuspended in growth medium (DMEM with 10% fetal bovine serum (FBS, Gibco), 100 units/ml penicillin, and 100 $\mu\text{g/ml}$ streptomycin), seeded on uncoated tissue-culture-treated polystyrene (TCPS), and cultured at 37°C and 5% CO_2 . Media was changed every 3 days.

Ultracentrifugation

In 15-fraction survey ("EV Isolation Optimization") or EV-enriched pooled fraction ("Tissue EV Vesiculomics") experiments, the 500xg supernatant from enzymatic digestion of cardiovascular tissues underwent further ultracentrifugation at 10,000xg for 10 minutes at 4°C (Beckman Coulter, Optima MAX-UP, fixed-angle rotor MLA-55) in 10 ml 16x76 mm polycarbonate uncapped centrifuge tubes (Beckman Coulter 355630). The resultant supernatant was collected and underwent ultracentrifugation at 100,000xg for 40 minutes at 4°C (rotor MLA-55) in 10.4 ml 16x76 mm polycarbonate capped centrifuge tubes (Beckman Coulter 355603), the pellet was washed once in PBS-/- and centrifuged again at 100,000xg for 40 minutes at 4°C . The final pellet was resuspended in 150 μl of NTE buffer (137 mM NaCl, 1 mM EDTA, 10 mM Tris, pH 7.4) with protease inhibitor (Roche, cOmplete Mini tablets, 4693159001). In ultracentrifugation library experiments, the 500xg supernatant was first spun at 10,000xg for 10 minutes at 4°C (Beckman Coulter, fixed angle rotor TLA 120.2) in 1 ml 11x34 mm polycarbonate uncapped centrifuge tubes (Beckman Coulter 343778), and the resultant supernatant was ultracentrifuged at 100,000xg for 40 minutes at 4°C (rotor TLA 120.2; Beckman Coulter 343778 1 ml uncapped tubes).

Density gradient centrifugation

In 15-fraction survey ("EV Isolation Optimization") or EV-enriched pooled fraction ("Tissue EV Vesiculomics") experiments, re-suspended ultracentrifugation-derived pellets were then layered onto the top of a linear 5-step 10-30% iodixanol gradient (composed of NTE buffer and OptiPrep Density Gradient Medium, Sigma-Aldrich D1556) in 10.4 ml 16x76 mm polycarbonate capped centrifuge tubes (Beckman Coulter 355603). The iodixanol gradient was then ultracentrifuged at 250,000xg for 40 minutes at 4°C (MLA-55), and 15 fractions were collected from the top of the gradient. In 15-fraction survey experiments ("EV Isolation Optimization"), each resultant fraction underwent separate ultracentrifugation at 100,000xg for 40 minutes at 4°C (rotor TLA 120.2) in 1 ml 11x34 mm polycarbonate uncapped centrifuge tubes (Beckman Coulter 343778). In EV-enriched pooled fraction experiments ("Tissue EV Vesiculomics"), fractions 1-4 were pooled together, topped up to a volume of 9 ml with NTE buffer, and underwent ultracentrifugation at 100,000xg for 40 minutes at 4°C (rotor MLA-55; Beckman Coulter 355603 10.4 ml capped tubes). Supernatant was discarded from each fraction, and the resultant pellets were re-suspended in buffers appropriate to their downstream applications (detailed below).

Transmission electron microscopy

5 µl of EVs (from iodixanol fraction(s) of interest, immediately after the 250,000xg density gradient centrifugation) were adsorbed for 1 minute onto carbon-coated, standard thickness, 400 mesh support film grids (EMS CF400-CU) made hydrophilic by plasma treatment (glow discharge, 25 mA). Excess liquid was removed with Whatman grade 1 filter paper (Sigma-Aldrich WHA1001325), and grids were rinsed of phosphate and salts by floating briefly on a drop of water. For immunogold labelling, samples were blocked with 1% bovine serum albumin (BSA) for 10 minutes, and incubated with primary antibody: mouse anti-human CD63 (BD Pharmingen 556019, 1:20 in 1% BSA), rabbit anti-human ITLN1 (Sigma-Aldrich HPA063275, 1:5), rabbit anti-human ENPP6 (Sigma-Aldrich HPA069197, 1:20), mouse anti-human PLVAP

(Abcam ab81719, 1:5), mouse anti-human PTK7 (Sigma-Aldrich WH0005754M2, 1:20), rabbit anti-human PLXNA4B (Abcam ab39350, 1:50), or rabbit anti-human NLGN4Y (Invitrogen PA5-120888, 1:20) for 30 minutes at room temperature. Grids were washed with 3 drops of PBS-/- in 10 minutes, then stained with rabbit anti-mouse bridging antibody (Abcam ab6709, 1:50 in 1% BSA) for 10 minutes. After further rinsing, grids were incubated with 10 nm Protein A-gold particles (University Medical Center Utrecht, 1:50 in 1% BSA) for 20 minutes. Samples were then washed in PBS-/- (2 changes in 5 minutes) and water (4 changes in 10 minutes). Grids were blotted again, then stained with 0.75% uranyl formate (EMS 22451) for 15 seconds. Excess uranyl formate was then removed by blotting, and grids were examined under a transmission electron microscope (JEOL 1200EX) and imaged with a CCD camera (AMT 2K).

Nanoparticle tracking analysis

Particle size and concentration was measured by nanoparticle tracking analysis (NTA, Malvern Instruments, NanoSight LM10). Before injection into the laser-illuminated chamber, samples were diluted 1:100 in PBS-/- (to $\sim 10^9$ particles/ml). For each sample, five data collection windows (1 minute per window) were recorded during continuous injection by a syringe pump (Malvern Instruments). Particles were detected and quantified at screen gain=1.0, camera level=9.0 for capture and screen gain=10.0 and detection threshold=2.0 for processing. Particle counts presented are the average of 5 collection windows. Particle size distributions are reported as the mean of all donors after sum normalization per donor. Data are presented as mean \pm standard error.

Protein quantification

In experiments where input to trypsin/RapiGest proteolysis or to the iST kit were normalized by protein amount (see below), protein yield was quantified by the bicinchoninic acid assay (BCA, Pierce 23225) on a NanoDrop 2000 spectrophotometer (Thermo Fisher Scientific) reading at 562 nm against a pre-mixed standard curve.

Proteomics sample preparation

To obtain peptides for mass spectrometry, whole-tissue samples were sonicated after RIPA lysis for 4 x 15 seconds (Branson Sonifier 450). Protein precipitation was performed by methanol-chloroform and proteolysis by trypsin/RapiGest (Promega Gold Grade, V5280/Waters RapiGest SF, 186001861) as described previously.⁵³ 15 µg of precipitated protein per sample was used for proteolysis. Tryptic peptides were desalted with Oasis HLB 1 cc/10 mg cartridges (Waters 186000383) and dried with a tabletop speed vacuum (Thermo Scientific SPD1010), then re-suspended in 40 µl of 5% mass spectrometry grade acetonitrile (Thermo Fisher Scientific) and 0.5% formic acid. EV samples were processed with the PreOmics iST kit (PreOmics GmbH, P.O.00027) according to the manufacturer's recommended protocol (v2.6), without sonication and with a 1.5-hour incubation at 37°C. Input to the iST kit varied by sample type. For 15-fraction survey experiments ("EV Isolation Optimization"), the pellet from each fraction was resuspended in 12 µl of LYSE, and 10 µl were loaded into the iST kit. EV pellets obtained by ultracentrifugation alone were each re-suspended in 12 µl of LYSE lysis buffer (PreOmics); 2 µl of the resultant solution was utilized for protein quantification by BCA, and a volume of LYSE equivalent to 5 µg of protein was loaded into the iST kit and topped up to 10 µl with additional LYSE. For EV-enriched pooled fractions ("Tissue EV Vesiculomics"), the pellet resulting from ultracentrifugation of pooled fractions 1-4 was re-suspended in 12 µl of LYSE; 2 µl of the resultant solution was utilized for protein quantification by BCA, and a volume of LYSE equivalent to 5 µg of protein was loaded into the iST kit and topped up to 10 µl with additional

LYSE. In all cases, peptides produced by the iST kit were resuspended in 40 μ l of LC-LOAD (PreOmics).

Mass spectrometry

Peptide samples were analyzed on an Orbitrap Fusion Lumos mass spectrometer fronted with an EASY-Spray Source (heated at 45°C), and coupled to an Easy-nLC1000 HPLC pump (Thermo Scientific). The peptides were subjected to a dual column set-up: an Acclaim PepMap RSLC C18 trap analytical column, 75 μ m X 20 mm (pre-column), and an EASY-Spray LC column, 75 μ m X 250 mm (Thermo Fisher Scientific). The analytical gradient was run at 300 nl/min, with Solvent A composed of water/0.1% formic acid and Solvent B composed of acetonitrile/0.1% formic acid). The acetonitrile and water were LC-MS-grade. For 30-minute gradients (ultracentrifugation libraries, stand-alone 15-fraction surveys), the analytical gradient was run from 5-21% Solvent B for 25 minutes and 21-30% Solvent B for 5 minutes. For 90-minute gradients (whole-tissue samples, ultracentrifugation libraries, EV-enriched pooled fractions), the analytical gradient was run from 5-21% Solvent B for 75 minutes and 21-30% Solvent B for 15 minutes. Whole-tissue samples (15 μ g input) were diluted 1:20 in loading buffer prior to injection. Stand-alone 15-fraction surveys were injected at 1X. Ultracentrifugation libraries (5 μ g input) and EV-enriched pooled fractions (5 μ g input) were diluted 1:2 in loading buffer prior to injection. The Orbitrap analyzer was set to 120 K resolution, and the top N precursor ions in 3 seconds cycle time within a scan range of 375-1500 m/z (60 seconds dynamic exclusion enabled) were subjected to collision induced dissociation (CID; collision energy, 30%; isolation window, 1.6 m/z; AGC target, 1.0 e4). The ion trap analyzer was set to a rapid scan rate for peptide sequencing (tandem mass spectrometry; MS/MS). When targeted mass exclusion of iodixanol was performed, it was enacted at an m/z of 775.8645 (z=2) with an exclusion mass width of 10 ppm. The retention time window was determined by pilot injections

for each sample type, with a 4-minute retention time window for the 30-minute gradients and a 7-minute window for the 90-minute gradient.

Whole-tissue comparisons of normal and disease stage-separated tissue (Figure S5): Peptide samples were analyzed with the high resolution/accuracy Q Exactive Orbitrap mass spectrometer fronted with a Nanospray FLEX ion source, and coupled to an Easy-nLC1000 HPLC pump (Thermo Scientific). The peptides were subjected to a dual column set-up: an Acclaim PepMap RSLC C18 trap column, 75 μ m x 20 mm; and an Acclaim PepMap RSLC C18 analytical column 75 μ m x 250 mm (Thermo Scientific). The analytical gradient was run at 300 nl/min from 5-18% Solvent B (acetonitrile/0.1% formic acid) for 120 minutes, followed by five minutes of 95% Solvent B. Solvent A was 0.1% formic acid. All reagents were HPLC-grade. Whole-tissue samples (15 μ g input) were diluted 1:20 in loading buffer prior to injection. The instrument was set to 140 K resolution, and the top 10 precursor ions (within a scan range of 380-2000 m/z) were subjected to higher energy collision-induced dissociation (HCD, collision energy 25% (+/- 2.5%), isolation width 1.6 m/z, dynamic exclusion enabled (20 seconds), and resolution set to 17.5 K).

Resultant whole-tissue MS/MS data were queried against the Human (UP000005640, downloaded November 21, 2018) UniProt database, and tissue-derived EV MS/MS data were queried against the Human (UP000005640, downloaded July 7, 2014 for stand-alone 15-fraction survey experiments or November 21, 2018 for all others), *Hathewayia histolytica* (May 16, 2018), and *Hathewayia proteolytica* (UP000183952, July 9, 2018) UniProt databases simultaneously, using the HT-SEQUEST search algorithm, via the Proteome Discoverer (PD) Package (version 2.2, Thermo Scientific). Whole-tissue staged MS/MS data were also merged per donor as fractions in PD 2.2 and re-processed as above for whole-tissue/EV proteome correlation analyses. Ultracentrifugation libraries were included in PD processing of 15-fraction

survey and EV-enriched pooled fraction experiments. Trypsin was set as the digestion enzyme while allowing up to four miss-cleavages, using 10 ppm precursor tolerance window and 0.6 Da (Lumos CID) or 0.02 Da (Q Exactive HCD) fragment tolerance window. Oxidation of methionine and N-terminus acetylation were set as variable modifications, and carbamidomethylation of cysteine was set as a fixed modification. The peptide false discovery rate (FDR) was calculated using Percolator provided by PD and peptides were filtered based on a 1.0% FDR.

Quantification utilized unique peptides (those assigned to a given Master protein group and not present in any other protein group) and razor peptides (peptides shared among multiple protein groups). Razor peptides were used to quantify only the protein with the most identified peptides and not for the other proteins they are contained in. A minimum of two unique peptides were required for a protein to be included in each dataset. To quantify peptide precursors detected in the MS1 but not sequenced from sample to sample, we enabled the 'Feature Mapper' node.

Chromatographic alignment was done with a maximum retention time (RT) shift of 10 minutes and a mass tolerance of 10 ppm. Feature linking and mapping settings were: RT tolerance minimum of 0 minutes, mass tolerance of 10 ppm and signal-to-noise minimum of 5. Precursor peptide abundance quantification was based on chromatographic intensities. For stand-alone 15-fraction survey experiments, there was no normalization of peptide amount/intensity. Total peptide amount was used for normalization in all other cases.

RNA isolation

In EV-enriched pooled fraction experiments ("Tissue EV Vesiculomics"), the pellet resulting from ultracentrifugation of pooled fractions 1-4 was re-suspended in 700 µl of TRIzol (Invitrogen 15596026). Samples were then vortexed for 1 minute, and total RNA was extracted using the miRNeasy Mini Kit (Qiagen 217004) according to the manufacturer's suggested protocol; each sample was eluted off the column twice using a total of 22 µl of RNase-free water.

Small RNA sequencing

Fragment analysis was performed on a Bioanalyzer 2100 (Agilent) using the Small RNA Analysis Kit (Agilent DNF-470-0275). cDNA libraries were synthesized with 3 ng of total RNA per sample input to the Clontech SMARTer smRNA-seq kit (Takara Bio 635034) using the manufacturer's suggested protocol. The finished libraries were quantified by Qubit fluorometer, Agilent TapeStation 2200, and RT-qPCR using the Kapa Biosystems library quantification kit according to manufacturer's protocols. Uniquely indexed libraries were pooled in equimolar ratios targeting 20M clusters per library and a single-ended 75bp high-output (75 cycle) sequencing run was performed on an Illumina NextSeq 500, to a target of 20 million reads per sample.

Bioinformatic analyses

Proteomics

Bacterial proteins (originating from the *Clostridium*-derived collagenase) were excluded. For whole-tissue samples ("Whole-Tissue Proteomics", "Supplemental Whole-Tissue Proteomics"), collagenase libraries, and EV-enriched pooled fractions ("Tissue EV Vesiculomics"), the quantified proteins were exported from Proteome Discoverer and median-normalized (per sample) using in-house scripts written in Python v3.4.^{21,54-57} Missing values were replaced with zero values in order to be analyzed by Qlucore Omics Explorer statistical software (Qlucore, v3.7): Thresholding of protein intensities was performed at level = 0.001, then intensities were log₂-transformed for subsequent statistical analysis. Significantly differentially-enriched proteins were calculated using a multi-group comparison (whole-tissue data; non-diseased vs. fibrotic vs. calcified stages; ANOVA: mixed-effects, single factor design) or two-group comparison (tissue

EV data; normal vs. diseased tissue EVs; ANOVA: independent measures, single factor design) at a Benjamini-Hochberg false discovery rate⁵⁸ (FDR, q or adjusted p -value) ≤ 0.05 . PCA and heat map analyses (z-score-based, ordered by hierarchical clustering) were performed on complete proteomes ($q \leq 1$). Per-protein normalized intensities from the overlapping portion of the merged whole-tissue and diseased tissue EV proteomes were averaged across donors, thresholded and transformed as above, then compared using linear regression and Pearson's r correlation coefficient. Correlation significance was assessed by a two-tailed p -value at a 95% confidence interval in Prism (GraphPad, v9).

Small RNA-Sequencing

Data were retrieved from the sequencer in the form of FASTQ files, and processed using the open-source bcbio.nextgen framework (github.com/bcbio/bcbio-nextgen). As per the Clontech SMARTer smRNA-seq kit instructions, the first three nucleotides from the template-switching oligo on the 5' end were trimmed prior to mapping, and a 10(A) adapter was identified and removed⁵⁹ by cutadapt.⁶⁰ STAR⁶¹ was used to perform sequence alignment with the human genome, and seqbuster detected small RNA transcripts.⁶²⁻⁶⁴ miRNAs were annotated using the miraligner tool with miRbase⁶⁵ as the reference miRNA database. Quality control was managed by FastQC.⁶⁶ After annotation, raw miR counts were normalized, transformed, and tested for statistically-significant differential expression using DESeq2¹⁶ defaults at an $FDR \leq 0.05$. PCA and heat map analyses (z-score-based, ordered by hierarchical clustering) were performed on the complete miRNAome ($q \leq 1$). We used TargetScan 7.2 to predict target genes for these EV miRs, with a high-confidence threshold of $\geq 95^{\text{th}}$ percentile weighted context++ score. After prediction of miR target genes, EV miRNA/mRNA target networks were generated in Gephi v0.9.2, where each differentially-enriched miR was connected to its predicted targets.

Gene ontology, gene set/pathway enrichment and network analyses

Using ConsensusPathDB,⁶⁷ gene sets were tested for enrichment by a hypergeometric test and adjusted for multiple comparisons using the Benjamini-Hochberg FDR. Pathways from BioCarta,⁶⁸ KEGG,⁶⁹ and Reactome⁷⁰ as well as gene ontology (GO) terms (retrieved from consensuspathdb.org in December 2019) with a p-value ≤ 0.05 were considered to be significantly-enriched in a gene set of interest. Significant overrepresentation of vesicle-associated GO terms in the disease-altered proteome shared by carotid artery and aortic valve whole tissues was assessed by comparing incidence of term names that included “vesicle” in the enriched terms list (21/1,105) vs. the total database (408/47,223) using a two-tailed Chi-square test at $p \leq 0.05$. GO term enrichment was assessed using terms found in the biological process, molecular function, and cellular component categories for all GO levels. Bubble plots of enriched “KEGG 2021 Human pathways” were generated by testing proteomics-derived gene sets for enrichment with Enrichr⁷¹ (retrieved in July 2022) at default settings. Coabundance profiling in 15-fraction survey experiments (“EV Isolation Optimization”) was performed using high-dimensional quantitative clustering in XINA (v3.9).^{22,52} Raw protein intensities from PD2.2 were normalized by total protein intensity per donor. Normalized protein abundances per OptiPrep fraction were merged into two tissue-specific datasets, each with three fraction ranges (F1-4, 5-10, 11-15) for subsequent clustering analyses. Coabundance patterns were fit to 10 clusters per analysis and functionality of cluster constituents was assessed by ConsensusPathDB as above.

Pathway networks are composed of pathways as the nodes and shared genes between pathways as the edges. Node size corresponds to $-\log(q\text{-value})$ and edge weight (thickness) corresponds to the gene overlap between pairs of pathways measured by the Jaccard index J , which is defined as

$$J = \frac{s_A \cap s_B}{s_A \cup s_B}$$

where s_A and s_B are the set of proteins detected in proteomics and gene targets of miRs detected in transcriptomics that belong to pathway A and pathway B , respectively. Edges with a Jaccard index < 0.1 were discarded in the visualization for clarity. Modularity optimization via the Louvain method¹⁷ was utilized to cluster pathway nodes into real network communities, overarching community functions were manually assigned, and standalone nodes were removed. The network visualizations were made using Gephi v0.9.2. Integrated pathway-specific PPI networks were produced by mapping the gene list that defined the pathway of interest from ConsensusPathDB onto the STRING v11.0¹⁸ PPI network (at a confidence score cutoff of 800). Nodes (and their shared edges) that were significantly enriched between normal and diseased tissues in the EV proteome or that were high-confidence targets of miRs significantly enriched between normal and diseased tissues in the EV miRNAome were highlighted. STRING v11.0 was also used at default settings with disconnected nodes hidden to generate protein-protein interaction networks, GO cellular component, UniProt Keyword, and KEGG pathway analyses of the impacts of OptiPrep density gradient separation and targeted mass exclusion on extracellular vesicle purification.

Cell culture experiments

Cell culture

Primary human adult carotid artery smooth muscle cells (hCtASMCs; Cell Applications Inc., 3514-05a; n=3 donors [donor IDs 2139, 2345, 3003]) were sub-cultured in Smooth Muscle Cell Growth Medium 2 (PromoCell, C-22162). Primary human adult valvular interstitial cells (hVICs; Lonza, 00225974; n=3 donors [donor IDs 1F266, 1F5026, 1F5079]) were sub-cultured in DMEM with 4.5 g/L glucose (Thermo Fisher Scientific, 10569010), 10% fetal bovine serum (FBS), and 1% penicillin/streptomycin (P/S). All experiments were performed on hCtASMCs from passage

6-7 and on hVICs from passage 2-3. When cells reached 90% confluence, two cell culture conditions were introduced as previously described:⁵² normal media (NM; DMEM with 4.5 g/L glucose, 5% FBS, and 1% P/S) or pro-calcifying media (PM; DMEM with 4.5 g/L glucose, 5% FBS, 1% P/S 5%, 2 mM NaH₂PO₄ [pH 7.4], 50 µg/mL L-ascorbic acid). siRNA experiments were performed without P/S addition to media.

siRNA knockdown

siRNA knockdown was performed by incubation with non-targeting scrambled siRNA and validated ON-TARGETplus siRNA (Horizon Discovery) or SilencerSelect siRNA (Thermo Fisher Scientific) for the indicated target genes with DharmaFECT 1 transfection reagent (Horizon Discovery):

Target	siRNA
siRNA Scr	Silencer Select; 4390843
FGFR2	ON-TARGETplus Human FGFR2 (2263) siRNA – SMARTpool; L-003132-00-0005
PPP2CA	Silencer Select; s10957, 4390824
ADAM17	Silencer Select; s13718, 4390824
WNT5A	ON-TARGETplus Human WNT5A (7474) siRNA – SMARTpool; L-003939-00-0005
APP	Silencer Select; s1500, 4390824
APC	Silencer Select; s1433, 4390824

The final in-well concentration of siRNA was adjusted to 20 nmol/L, and siRNA transfection was performed according to the manufacturer's protocol. hCtASMCs and hVICs were seeded at day -4 in NM (5 days before media exchange to PM) at 0.6×10^5 cells/ml. The first transfection of siRNA was performed the following day in NM media (day -3). At day 0, media was switched from NM to PM (or continued with NM for controls) with appropriate siRNA addition. After day 0, media exchange and transfection of siRNA were performed every 3 days.

Quantitative real-time PCR

Validation of RNA silencing was performed in hCtASMCs and hVICs as relevant. RNA was collected from cells cultured in NM in 24-well plates using TRIzol reagent (Thermo Fisher Scientific Inc., 15596-018) at day 6 and total RNA was extracted as per the manufacturer's protocol. 1 µg of total RNA from each sample was reverse transcribed using the qScript cDNA Synthesis Kit (Quantabio, 95047) according to the manufacturer's protocol. PCR reactions were performed using PerfeCTa® qPCR FastMix® II, ROX™ (Quantabio, 95119) and TaqMan Gene Expression Assays (VIC/FAM):

Gene	Sequence #	Catalog #
GAPDH	Hs02758991_g1	4331182
FGFR2	Hs01552918_m1	4453320
PPP2CA	Hs00427259_m1	4453320
ADAM17	Hs01041915_m1	4453320
WNT5A	Hs00998537_m1	4453320
APP	Hs00169098_m1	4453320
APC	Hs01568269_m1	4453320

Quantitative real-time PCR was performed on a QuantStudio 5 Real-Time PCR System (Thermo Fisher Scientific). After linear range was determined using a standard curve from a dilution series of all pooled samples, the relative value of mRNA abundance was quantified by delta-delta Ct vs. the housekeeping gene GAPDH. N=1 donor per cell type, triplicate wells per donor, duplicate qPCR reactions were averaged per well.

Alizarin red staining

To assess calcification, hCtASMCs (n=3 donors) and hVICs (n=3 donors) cultured in duplicate in 48-well plates in NM or PM and treated with siRNA were stained by Alizarin red at days 14 and 21. Briefly, cells were washed with PBS-/-, fixed with 4% formaldehyde for 10 minutes, then stained with 2% Alizarin Red Stain (Lifeline Cell Technology, CM-0058) for 20 minutes and images were scanned from the bottom of culture plates. Staining intensity was quantified using 100 mM cetylpyridinium chloride solubilization (Thermo Fisher Scientific Inc.) for 3 hours and subsequent spectrophotometric assessment at OD 540; technical duplicates were averaged per timepoint per donor.

Histology

Representative longitudinal (tip-to-base; AV leaflets) or cross-sectional (carotid artery) tissue segments were embedded in OCT compound (Tissue-Tek), and 7 μ m cryosections were cut using a cryostat (Research Cryostat, Leica CM3050 S). To assess disease, sections were stained by hematoxylin and eosin (H&E) and von Kossa (VK). In brief, H&E staining was performed by drying sections for 30 minutes, followed by post-fixing in formalin for 10 minutes. After rinsing, sections were stained in Harris hematoxylin (Shandon, Thermo Scientific) for 2 minutes, dipped three times in acetic acid, stained for 1 minute in ammonium water, rinsed in 70% ethanol, stained in 1% alcoholic eosin (VWR) for 1 minute with agitation, and dehydrated in 95% ethanol, 100% ethanol, and xylene prior to coverslipping in SHUR/Mount (VWR). VK staining was performed by drying sections for 20 minutes, followed by post-fixing in formalin for 10 minutes. After rinsing, sections were stained in 5% silver nitrate (Abcam) under UV light for 60 minutes, treated with 5% sodium thiosulfate (Abcam) for 3 minutes, counterstained in Nuclear Fast Red (Abcam) for 5 minutes, and dehydrated in 100% ethanol and xylene prior to coverslipping in SHUR/Mount (VWR). Stained sections were imaged using a Nikon 50i microscope and Nikon NIS Elements AR v. 3.10. Three sections per donor were scored on a

quantitative histopathological scoring index with a scale of 0 to 3 (none, mild, moderate, severe) for inflammation, fibrosis, and calcification (and summed as an overall disease score) by a trained pathologist who was blinded to disease stage/status.

Statistical Analysis

Statistical analyses of non-omics datasets was performed via Student's *t*-test (two-tailed, (un)paired as appropriate) for comparisons between two groups; one-way or two-way ANOVA with/without mixed-effects as appropriate with Holm-Sidak post-hoc multiple comparisons tests were used to evaluate statistically significant differences in multiple group comparisons. Fisher's exact test or multiple logistic regression assessed prevalence as appropriate (GraphPad Prism v9). In brief, plaque-valve PCA centroid distances were assessed by one-way mixed-effects ANOVA ("Whole-Tissue Proteomics"). Prevalence of vesicle GO terms was examined by Fisher's exact test ("Whole-Tissue Proteomics"). Testing of siRNA knockdown efficacy employed Student's *t*-test (two-tailed, unpaired), while quantification of *in vitro* alizarin red calcification utilized Student's *t*-test (two-tailed, paired). Histological stains were assessed by two-way ANOVA with (diseased stage-separated) or without (normal vs. diseased) mixed-effects. Donor age characteristics were compared between groups using a one-way ("Whole-Tissue Proteomics") or two-way ("Supplemental Whole-Tissue Proteomics"; "Tissue EV Vesiculomics") ANOVA. ANOVA multiple comparisons testing was performed with the Holm-Sidak post-hoc method. Donor sex characteristics were assessed between groups using a Fisher's exact test ("Whole-Tissue Proteomics") or multiple logistic regression analysis ("Supplemental Whole-Tissue Proteomics"; "Tissue EV Vesiculomics").

Table S1: ProteomeXchange Consortium/PRIDE repository proteomics datasets.

Dataset	Accession	DOI
Whole Tissue (ND/F/C; F2)	PXD035538	10.6019/PXD035538
15-Fraction Surveys (F3, S12)	PXD035580	10.6019/PXD035580
Tissue EVs (F4, S19)	PXD035529	10.6019/PXD035529
Whole Tissue (merged; F4C)	PXD035563	10.6019/PXD035563
Supplemental Whole Tissue (N/ND/F/C; S7)	PXD035555	10.6019/PXD035555
UC vs. OptiPrep (S15)	PXD035485	10.6019/PXD035485
Iodixanol Exclusion (S16-17)	PXD035505	10.6019/PXD035505

Table S2: Available baseline characteristics of the tissue donors.

A. Whole Tissue Proteomics

	Diseased Carotid Artery (n=8)	Diseased Aortic Valve (n=18)	p-value
Donor age, years	71 ± 10	69 ± 7	0.5130
Male sex, %	75.0%	77.8%	>0.9999

Values are mean ± standard deviation (age) or % prevalence (male sex).

B. Supplemental Whole-Tissue Proteomics

tissue type (t):	Carotid Artery		Aortic Valve		
disease status (d):	Normal (n=3)	Diseased (n=7)	Normal (n=5)	Diseased (n=9)	p-value
Donor age, years	73 ± 5	71 ± 10	71 ± 7	70 ± 7	0.6889 (t) 0.7008 (d)
Male sex, %	66.7%	71.4%	80.0%	66.7%	0.6760 (t) 0.8804 (d)

Values are mean ± standard deviation (age) or % prevalence (male sex).

Donor age *p*-values are reported by tissue type (top) and disease status (bottom) factors.

C. Tissue EV Vesiculomics

tissue type (t):	Carotid Artery		Aortic Valve		
disease status (d):	Normal (n=6)	Diseased (n=4)	Normal (n=6)	Diseased (n=4)	p-value
Donor age, years	70 ± 15	74 ± 6	73 ± 8	65 ± 9	0.5494 (t) 0.6542 (d)
Male sex, %	66.7%	100%	83.3%	75.0%	>0.9999 (t) 0.5013 (d)

Values are mean ± standard deviation (age) or % prevalence (male sex).

Donor age *p*-values are reported by tissue type (top) and disease status (bottom) factors.

List of Supplemental Tables S3-S46 (found in Supplemental Excel File I)

Table S3: Proteins changed by disease progression in carotid whole tissue

Table S4: Proteins changed by disease progression in aortic valve whole tissue

Table S5: Volcano proteins changed by disease progression only in carotid whole tissue

Table S6: Pathways of proteins changed by disease progression only in carotid whole tissue

Table S7: Network scores of proteins changed by disease progression only in carotid whole tissue

Table S8: Volcano proteins changed by disease progression only in aortic valve whole tissue

Table S9: Pathways of proteins changed by disease progression only in aortic valve whole tissue

Table S10: Network scores of proteins changed by disease progression only in aortic valve whole tissue

Table S11: Venn proteins changed by disease progression only in carotid or aortic valve whole tissues or both

Table S12: GO terms of proteins changed by disease progression in carotid and aortic valve whole tissues

Table S13: Pathways of proteins changed by disease progression in carotid and aortic valve whole tissues

Table S14: Network scores of proteins changed by disease progression in carotid and aortic valve whole tissues

Table S15: GO terms of proteins in selected XINA clusters from carotid OptiPrep F1-4

Table S16: GO terms of proteins in selected XINA clusters from aortic valve OptiPrep F1-4

Table S17: Cellular GO terms of proteins unique to ultracentrifugation

Table S18: UniProt keywords of proteins unique to ultracentrifugation

Table S19: Cellular GO terms of proteins unique to OptiPrep F1-4

Table S20: UniProt keywords of proteins unique to OptiPrep F1-4

Table S21: Pathways of proteins unique to targeted mass exclusion of OptiPrep fractions

Table S22: Proteins changed by disease progression in carotid EVs

Table S23: Proteins changed by disease progression in aortic valve EVs

Table S24: Venn proteins changed by disease progression only in carotid or aortic valve EVs or both

Table S25: KEGG pathways of proteins changed by disease progression in carotid or aortic valve EVs or both

Table S26: Pathways of proteins changed by disease progression only in carotid EVs

Table S27: Pathways of proteins changed by disease progression only in aortic valve EVs

Table S28: Pathways of proteins changed by disease progression in carotid and aortic valve EVs

Table S29: Proteins changed between carotid and aortic valve EVs

Table S30: Tissue EV small RNA-seq raw counts

Table S31: miRs changed by disease progression in carotid EVs

Table S32: miRs changed by disease progression in aortic valve EVs

Table S33: Venn miRs changed by disease progression only in carotid or aortic valve EVs or both

Table S34: High-confidence gene targets of miRs changed by disease progression only in carotid EVs

Table S35: High-confidence gene targets of miRs changed by disease progression only in aortic valve EVs

Table S36: High-confidence gene targets of miRs changed by disease progression in carotid and aortic valve EVs

Table S37: Network scores of miRs/targets changed by disease progression only in carotid EVs

Table S38: Network scores of miRs/targets changed by disease progression only in aortic valve EVs

Table S39: Network scores of miRs/targets changed by disease progression in carotid and aortic valve EVs

Table S40: KEGG pathways of gene targets of miRs changed by disease progression in carotid or aortic valve EVs or both

Table S41: Pathways of targets of miRs changed by disease progression only in carotid EVs

Table S42: Pathways of targets of miRs changed by disease progression only in aortic valve EVs

Table S43: Pathways of targets of miRs changed by disease progression in carotid and aortic valve EVs

Table S44: Network scores of protein and miR gene target pathways changed by disease progression in carotid and aortic valve EVs

Table S45: Network scores of integrated carotid EV-derived target pathways

Table S46: Network scores of integrated aortic valve EV-derived target pathways

Figure S1: Detailed Study Roadmap and Comprehensive Overview. Whole-Tissue

Proteomics was conducted on 3 stages of disease (paired non-diseased, fibrotic, and calcified regions per donor) dissected from specimens excised by carotid endarterectomy (due to carotid artery stenosis; n=16) and aortic valve replacement (due to aortic valve stenosis; n=18).

Proteomics was performed on a Thermo Orbitrap Fusion Lumos mass spectrometer.

Supplemental Whole-Tissue Proteomics was conducted on i) intact normal specimens (n=3 carotid arteries from autopsy, n=5 aortic valves from heart transplants; no dissection of disease stages/regions), and ii) 3 stages of disease (paired non-diseased, fibrotic, and calcified regions per donor) dissected from specimens excised by carotid endarterectomy (due to carotid artery stenosis; n=12) and aortic valve replacement (due to aortic valve stenosis; n=9). The carotid artery stenosis donors and aortic valve stenosis donors included in this analysis are sub-sets of the 16 carotid artery stenosis donors and 18 aortic valve stenosis donors presented in the “Whole-Tissue Proteomics” study. Proteomics was performed on a Thermo Q Exactive Orbitrap mass spectrometer. **EV Isolation Optimization** was conducted on intact specimens (no dissection of disease stages/regions). Specimens were excised by carotid endarterectomy (due to carotid artery stenosis; n=3) and aortic valve replacement (due to aortic valve stenosis; n=4). Proteomics was performed on a Thermo Orbitrap Fusion Lumos mass spectrometer. These donors are a different cohort than those included in the “Whole-Tissue Proteomics” or “Tissue EV Vesiculomics” sub-studies. **Tissue EV Vesiculomics** was conducted on intact specimens (no dissection of disease stages/regions). Normal specimens originated from autopsy (normal carotid arteries [n=6] and normal aortic valves [n=6]), while diseased samples were excised by carotid endarterectomy (due to carotid artery stenosis; n=4) and aortic valve replacement (due to aortic valve stenosis; n=4). Proteomics was performed on a Thermo Orbitrap Fusion Lumos mass spectrometer. These donors are a different cohort than those included in the “Whole-Tissue Proteomics” or “EV Isolation Optimization” sub-studies.”

■ Normal (N)
 ■ Diseased (D)
 ■ Non-Diseased (ND)
 ■ Fibrotic (F)
 ■ Calcified (C)

Whole-Tissue Proteomics

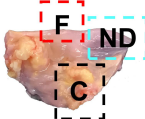
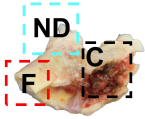
>> Fig. 2; S5, S6, S8-S10 <<

Carotid Artery

Aortic Valve

Diseased
(plaque)

Diseased
(calcified)

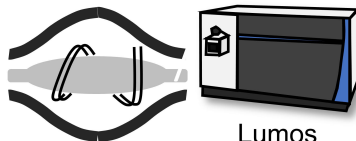


n = 16 x 3 stages

n = 18 x 3 stages

segmented by disease stage

Proteomics



Lumos

EV Isolation Optimization

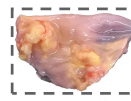
>> Fig. 3; S11-S15 <<

Carotid Artery

Aortic Valve

Diseased
(plaque)

Diseased
(calcified)



n = 3

n = 4

intact sample

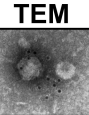
Dissection

Enzymatic
Digestion &
Centrifugation

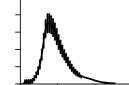
Ultra-
centrifugation

OptiPrep
Density
Gradient

F1-15



NTA



Proteomics



Tissue EV Vesiculomics

>> Fig. 4-7; S16-S26 <<

Carotid Artery

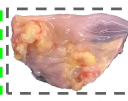
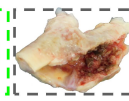
Aortic Valve

Normal
(autopsy)

Diseased
(plaque)

Normal
(autopsy)

Diseased
(calcified)



n = 6

n = 4

n = 6

n = 4

intact sample

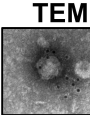
Dissection

Enzymatic
Digestion &
Centrifugation

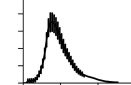
Ultra-
centrifugation

OptiPrep
Density
Gradient

F1-4



NTA



Proteomics



Small RNA-seq



Supplemental Whole-Tissue Proteomics

>> Fig. S7 <<

Carotid Artery

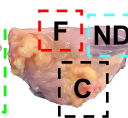
Aortic Valve

Normal
(autopsy)

Diseased
(plaque)

Normal
(heart tx)

Diseased
(calcified)



n = 3

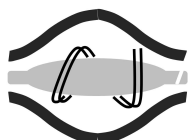
n = 12
x 3 stages

n = 5

n = 9
x 3 stages

Normals intact; Diseased segmented by disease stage

Proteomics

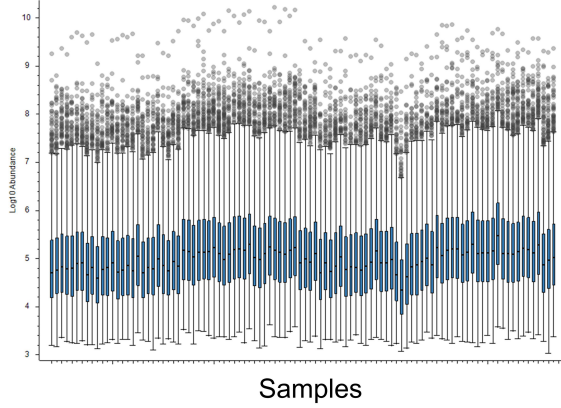
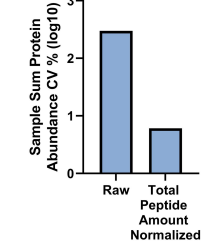
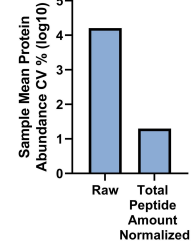
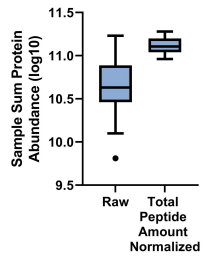
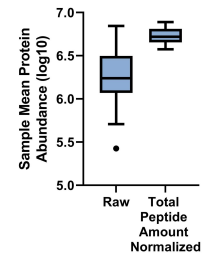
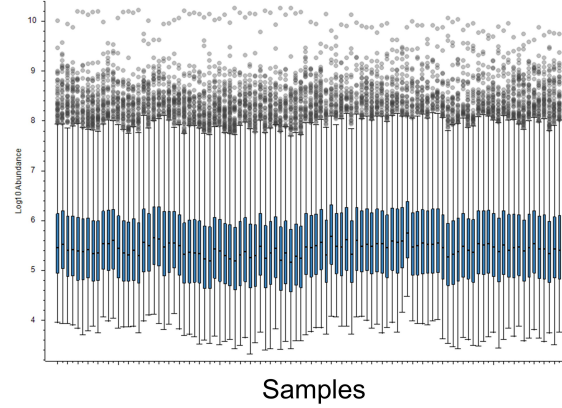


Q Exactive

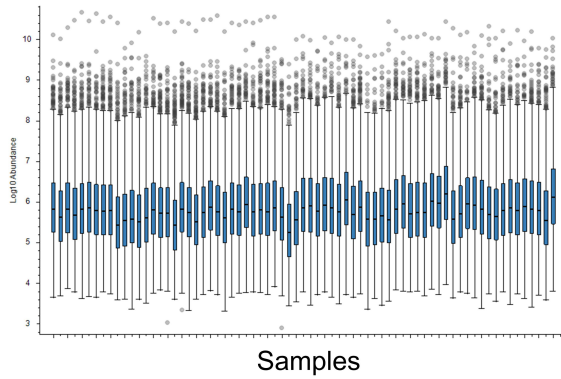
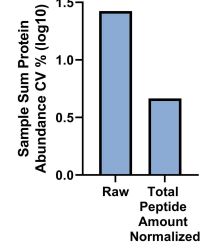
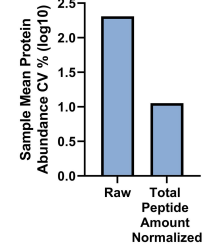
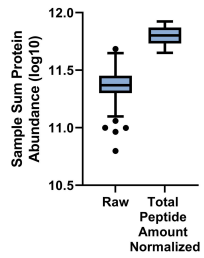
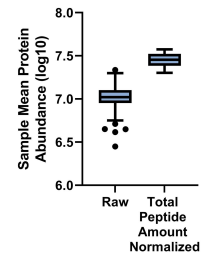
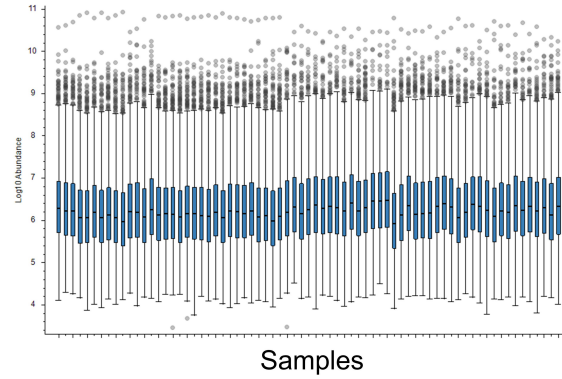
Figure S2: Proteome-Wide Between-Sample Normalization by Total Peptide Amount. Per-sample boxplots of raw protein abundances (left), protein abundances normalized between samples by leveraging the entire detected/quantified proteome via the Proteome Discoverer “Total Peptide Amount” normalization processing node (middle), and boxplots of per-sample mean protein abundance, sum protein abundance, CV % of per-sample mean protein abundance, and CV % of per-sample sum protein abundance for **A**, Whole Tissue Proteomics (Figure 2), **B**, Supplemental Whole-Tissue Proteomics (Figure S7), and **C**, Tissue EV Proteomics (Figure 4); abundances = log-transformed, box = median and IQR (interquartile range), whiskers = ± 1.5 IQR.

A

Whole-Tissue Proteomics

Protein Abundances (Raw)**Protein Abundances (Total Peptide Amount Normalized)****B**

Supplemental Whole-Tissue Proteomics

Protein Abundances (Raw)**Protein Abundances (Total Peptide Amount Normalized)****C**

Tissue EV Proteomics

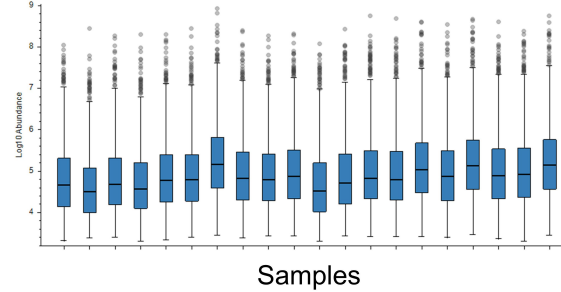
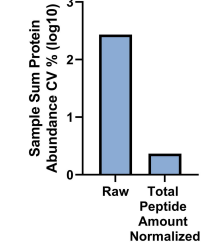
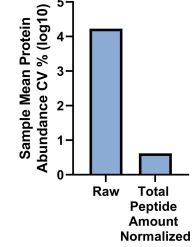
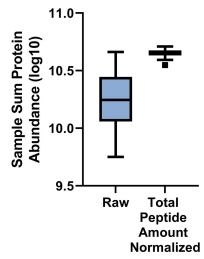
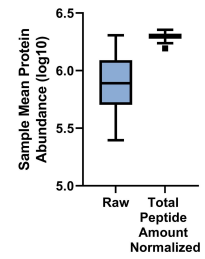
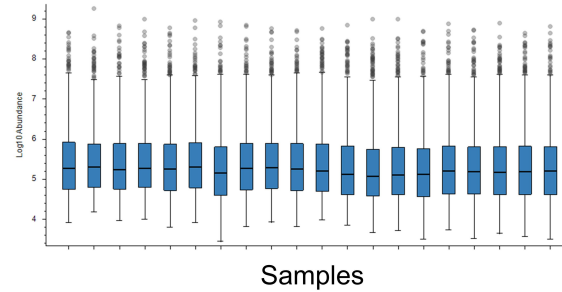
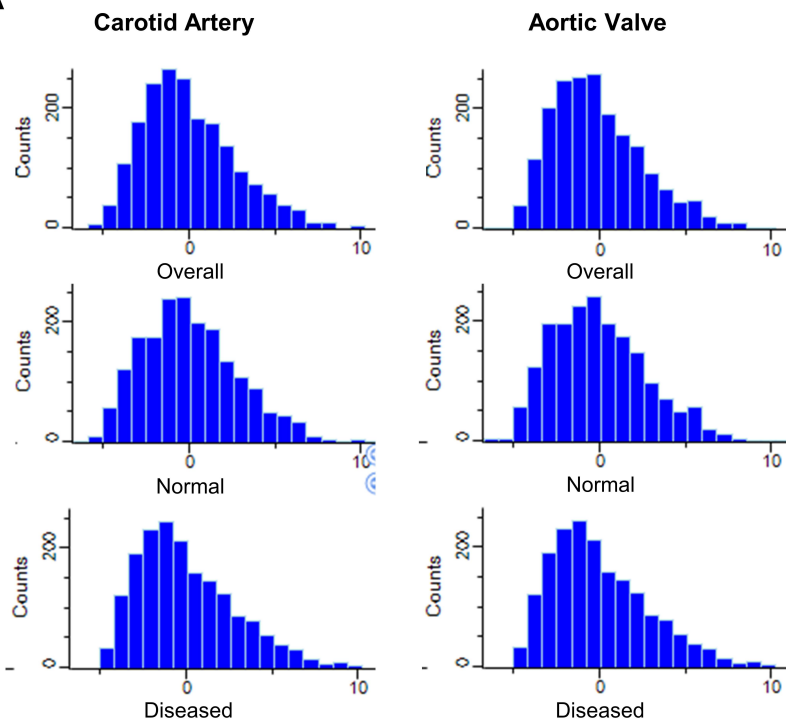
Protein Abundances (Raw)**Protein Abundances (Total Peptide Amount Normalized)**

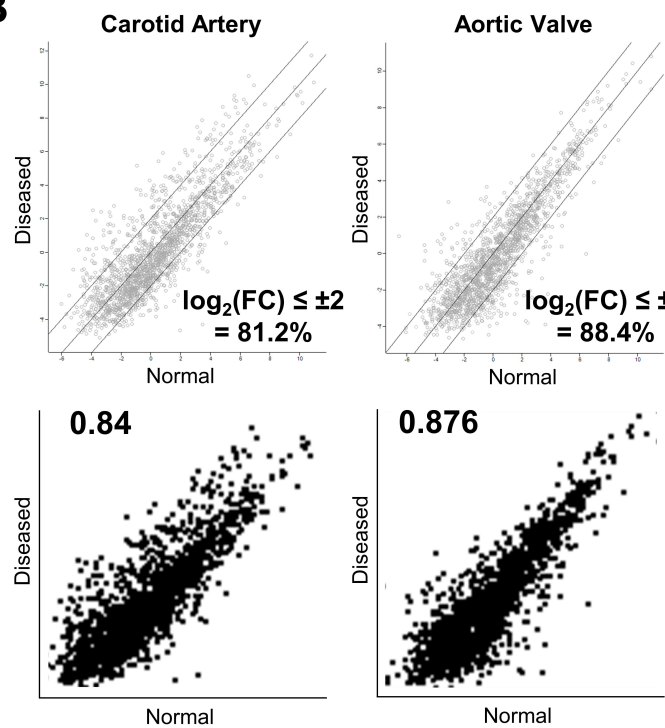
Figure S3: Quality Control of Primary Proteomics Datasets. A and C, Frequency distribution histograms of mean per-protein abundances (by sample group) after between-sample Total Peptide Amount normalization, within-sample median normalization, and \log_2 -transformation (A = “Tissue EV Proteomics”: tissue EVs from intact normal carotid arteries (n=6 donors), intact diseased carotid artery atherosclerotic plaques (n=4), intact normal aortic valves (n=6), and intact diseased calcified aortic valves (n=4), corresponds to Figure 4; C = “Whole-Tissue Proteomics”: n=16 carotid artery plaque and 18 calcified aortic valve donors x 3 stages of disease (non-diseased, fibrotic, calcified) per donor, corresponds to Figure 2). **B,** Top: pair-wise \log_2 (fold change) scatterplots of normal vs. diseased tissue EV proteins (after between-sample/within-sample normalization and \log_2 transformation). Lines indicate $y=x$, $x+2$, $x-2$. Bottom: pair-wise scatterplots of normal vs. diseased tissue EV mean protein abundances (by sample group, after between-sample/within-sample normalization and \log_2 transformation) with associated Pearson correlation coefficients. N=6 intact normal carotid arteries, n=4 intact diseased carotid arteries, n=6 intact normal aortic valves, n=6 intact diseased calcified aortic valves, corresponds to Figure 4. **D,** Pair-wise scatterplots of disease stage-specific whole-tissue mean protein abundances (by sample group, after between-sample/within-sample normalization and \log_2 transformation) with associated Pearson correlation coefficients. N=16 carotid artery plaque and 18 calcified aortic valve donors x 3 stages of disease (non-diseased, fibrotic, calcified) per donor, corresponds to Figure 2).

Tissue EV Proteomics

A

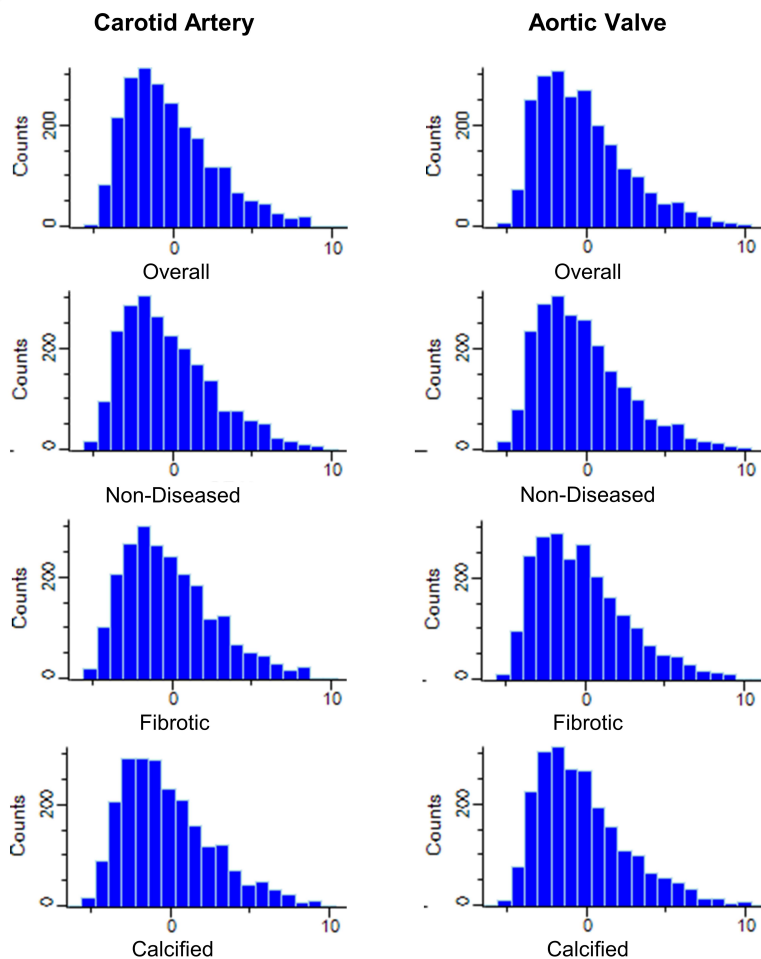


B



Whole-Tissue Proteomics

C



D

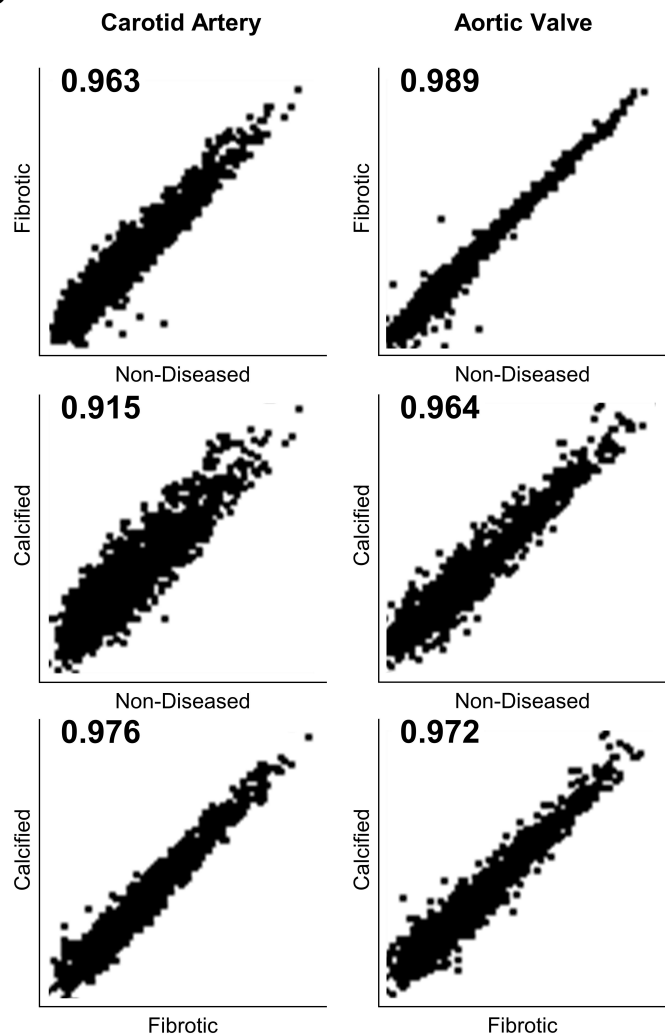
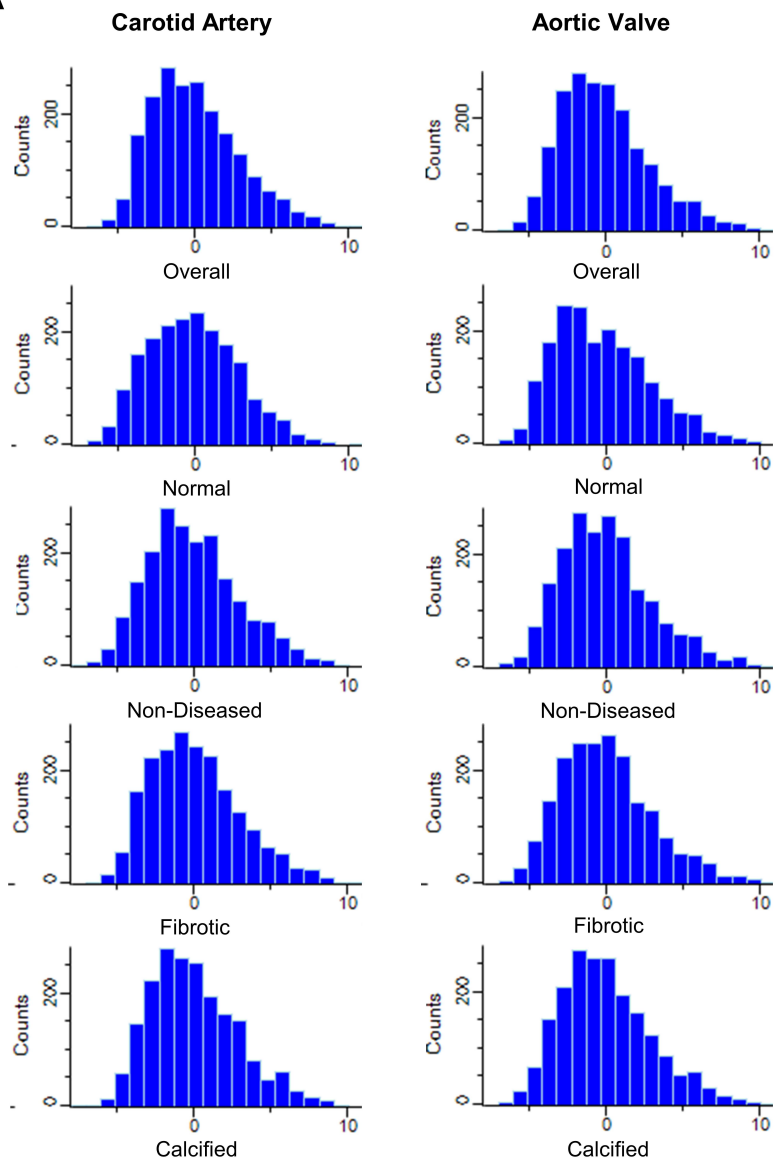


Figure S4: Quality Control of Supplemental Proteomics Dataset. **A**, Frequency distribution histograms of mean per-protein abundances (by sample group) after between-sample Total Peptide Amount normalization, within-sample median normalization, and \log_2 -transformation (“Supplemental Whole-Tissue Proteomics”: intact normal specimens (n=3 carotid arteries from autopsy, n=5 aortic valves from heart transplants) and n=12 carotid artery plaque and 9 calcified aortic valve donors x 3 stages of disease (non-diseased, fibrotic, calcified) per donor, corresponds to Figure S7). **B**, Pair-wise scatterplots of disease stage-specific whole-tissue mean protein abundances (by sample group, after between-sample/within-sample normalization and \log_2 transformation) with associated Pearson correlation coefficients. Intact normal specimens (n=3 carotid arteries from autopsy, n=5 aortic valves from heart transplants) and n=12 carotid artery plaque and 9 calcified aortic valve donors x 3 stages of disease (non-diseased, fibrotic, calcified) per donor, corresponds to Figure S7.

Supplemental Whole-Tissue Proteomics

A



B

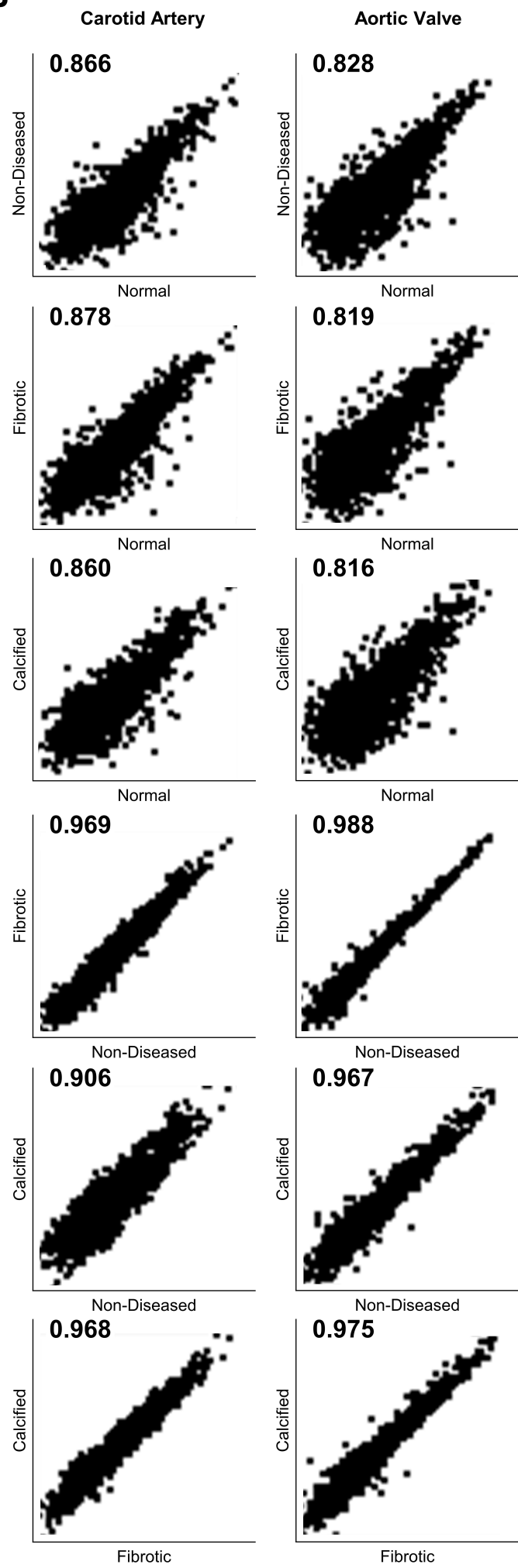
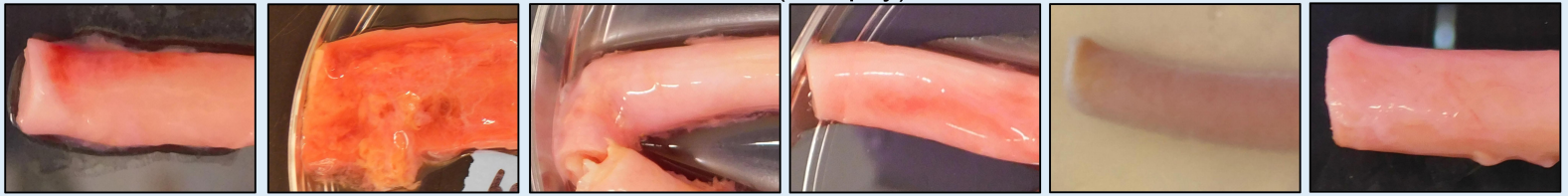


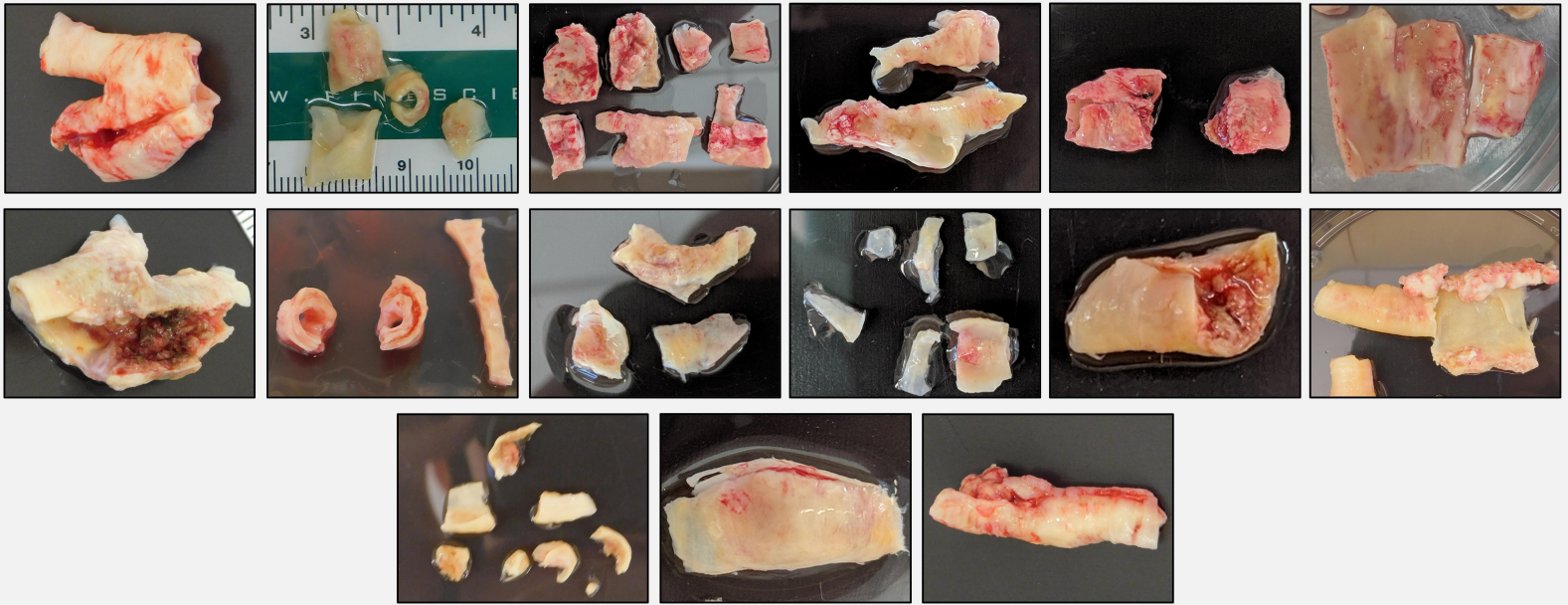
Figure S5: Tissue Gross Morphology. Images of gross morphology and pathology of available normal (acquired from autopsy) and diseased human carotid artery (acquired from carotid endarterectomies due to carotid artery stenosis) and aortic valve (acquired from valve replacement surgeries due to AV stenosis) tissues utilized in this study.

Carotid Artery

Normal (autopsy)

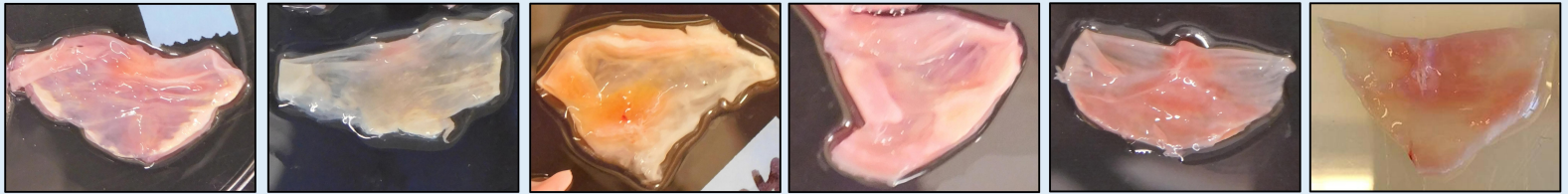


Diseased (plaque)



Aortic Valve

Normal (autopsy)



Diseased (calcified)

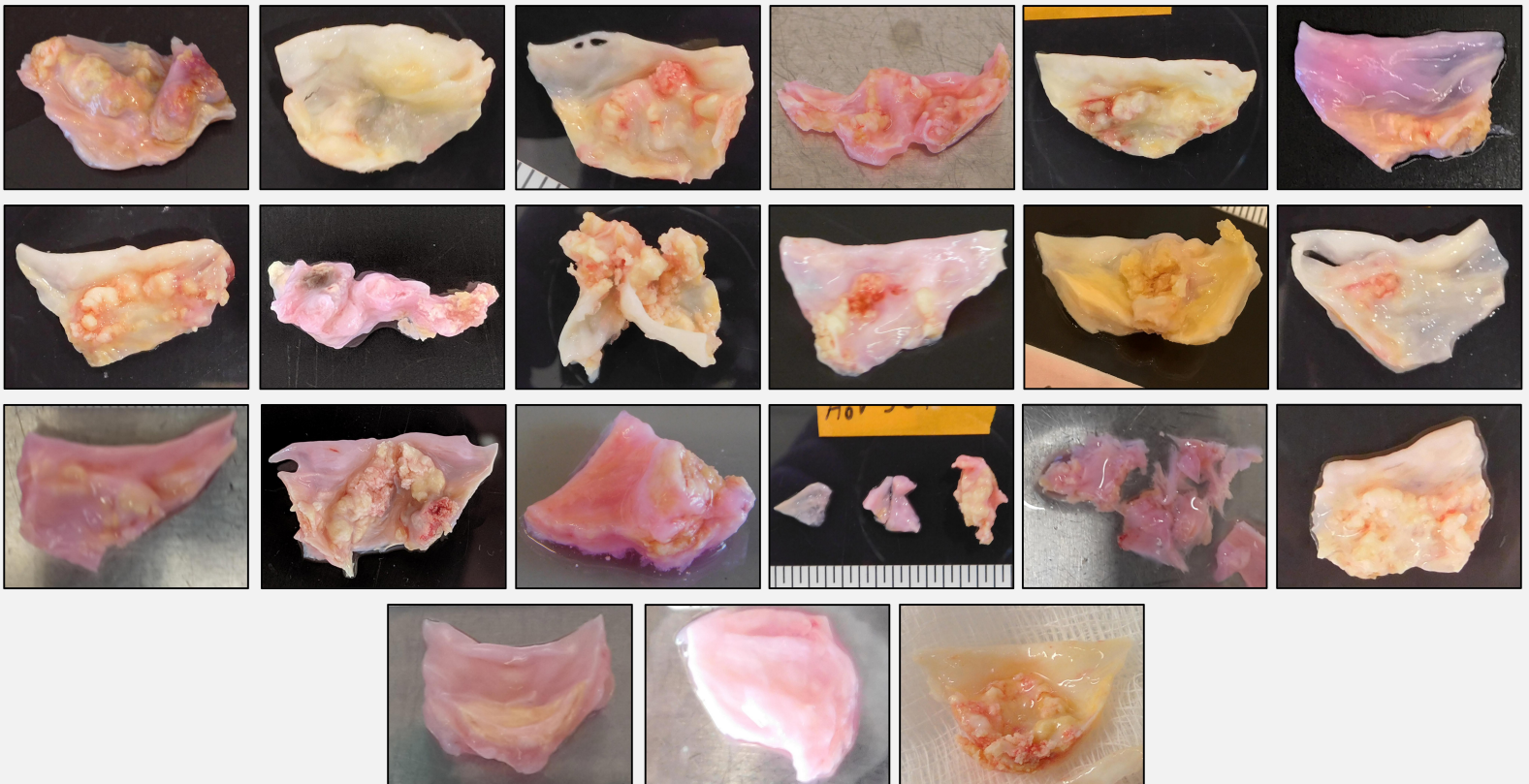


Figure S6: Histology of Tissue Disease Stages. A and B, Representative histological staining of disease stage-separated (non-diseased, fibrotic, calcified) carotid artery plaque cross-sections and calcified aortic valve longitudinal (tip-to-base) sections by hematoxylin and eosin for morphology and pathology (**A**, H&E) and von Kossa (**B**) for calcification. All scale bars = 200 μm . L = lumen, F = fibrosa, V = ventricularis. **C**, Quantitative histopathological score indices (0-3, none/mild/moderate/severe; summed for overall disease) for inflammation, fibrosis, calcification, and overall disease of 3 sections per stain per donor demonstrated i) minimal histological markers of disease in non-diseased stages, ii) sequential and significant increases in histological disease burden between disease stages indicating accurate stage-specific separation, and iii) no significant differences in histological disease burden between carotid artery and aortic valve tissue types at each stage of disease. Box plots 25th-75th percentiles; line = median; “+” = mean; whiskers represent minimum and maximum values; n=6 donors per group; * $p < 0.05$, ** $p < 0.01$, *** $p < 0.001$, **** $p < 0.0001$.

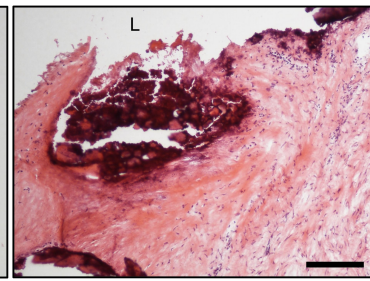
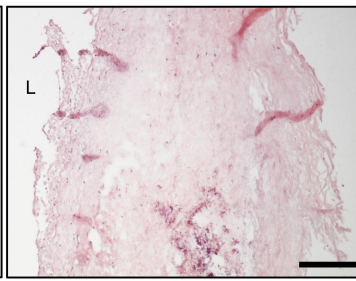
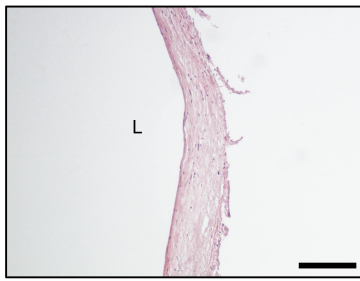
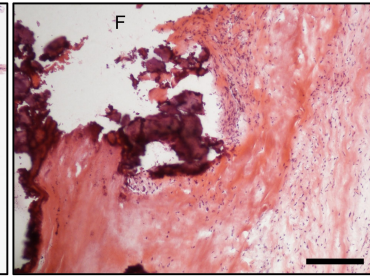
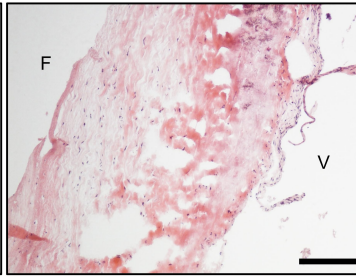
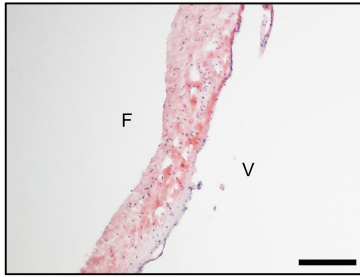
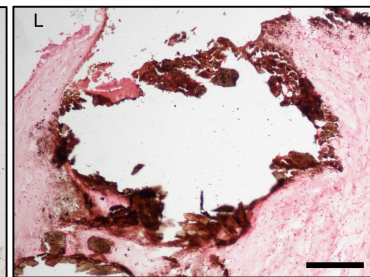
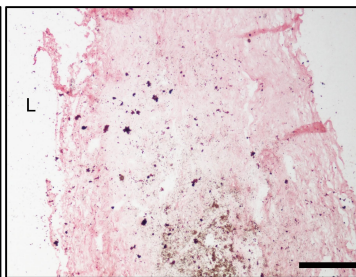
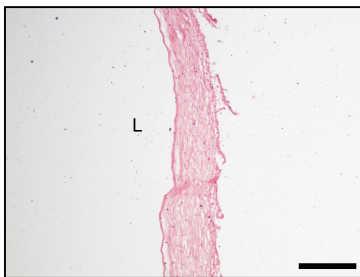
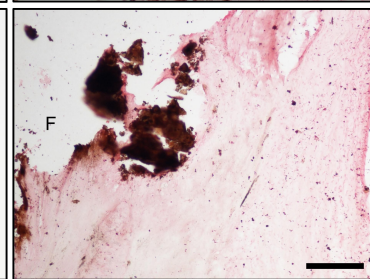
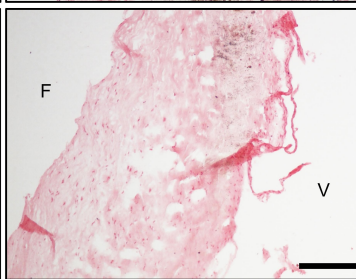
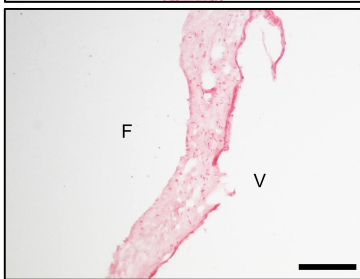
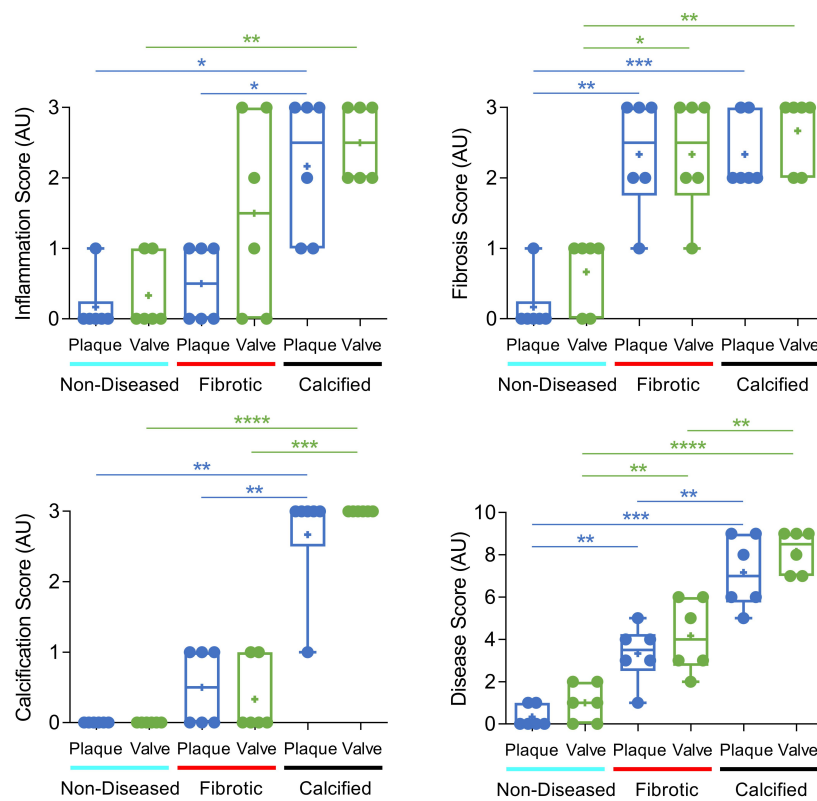
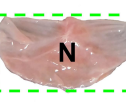
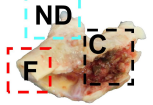
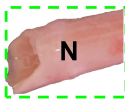
A**H&E****Non-Diseased****Fibrotic****Calcified****Carotid Artery
Plaque****Calcified
Aortic Valve****B****Von Kossa****Non-Diseased****Fibrotic****Calcified****Carotid Artery
Plaque****Calcified
Aortic Valve****C**

Figure S7: Whole Tissue Proteome of Normal and Diseased Tissues. **A**, Human label-free stage-specific proteomics was conducted on intact normal carotid arteries from autopsy (n=3), intact normal aortic valves from heart transplant recipients (n=5), and disease stage-separated carotid artery plaques (n=12) and calcified aortic valves (n=9) x 3 stages of disease per donor (non-diseased, fibrotic, calcified). **B-E**, The whole-tissue proteome was composed of 2,037 quantified proteins. Unfiltered principal component analyses ($q \leq 1$) identified distinct **(B)** tissue- and **(C)** disease state-specific (right) clustering. Normal samples (N) congregated within a larger non-diseased stage (ND) cluster in **(C)** overall, **(D)** carotid artery- and **(E)** aortic valve-specific analyses, with sequential spatial tracks leading from the normal/non-diseased co-cluster towards the fibrotic and then calcified clusters.

A**Whole Tissue Proteome (2,037 proteins, $q \leq 1$)**
 n = 29
Carotid Artery**Aortic Valve****Normal**
(autopsy)**Diseased**
(plaque)**Normal**
(heart tx)**Diseased**
(calcified)

n = 3

n = 12
x 3 stages

n = 5

n = 9
x 3 stages
 Carotid Artery

 Aortic Valve

 Normal (N)

 Non-Diseased (ND)

 Fibrotic (F)

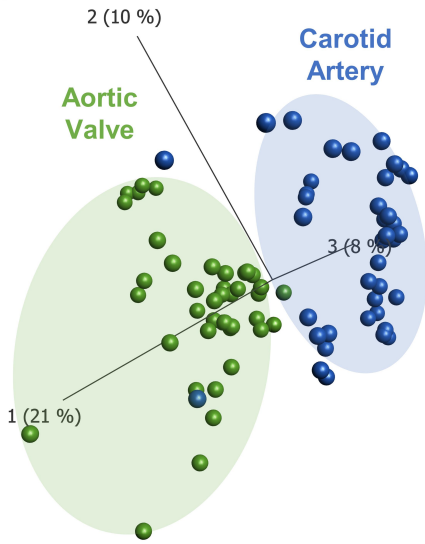
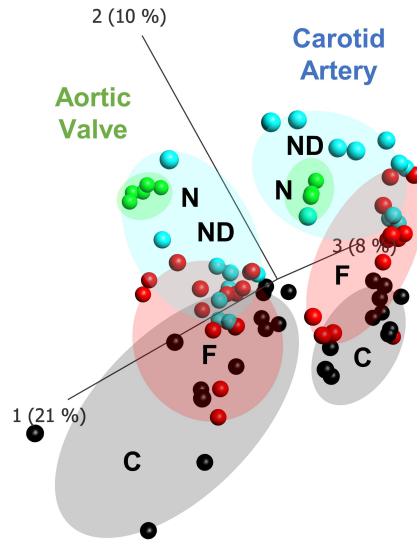
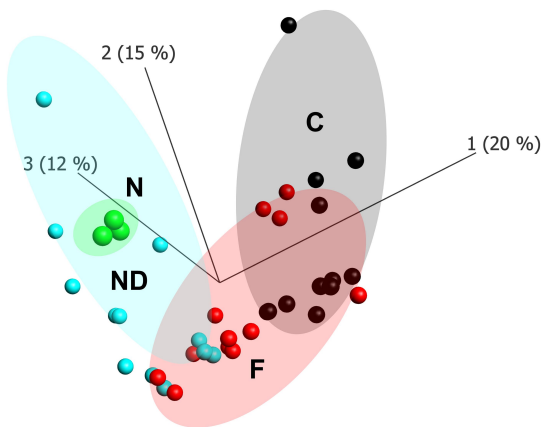
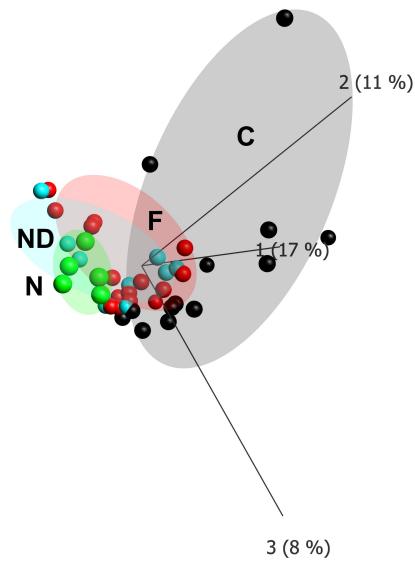
 Calcified (C)
B**C****D****Carotid Artery****E****Aortic Valve**

Figure S8: Labelled Network of Disease-Altered Pathways in Carotid Artery Whole

Tissue. Network based on KEGG, Reactome, and BioCarta pathway enrichment among proteins significantly differentially enriched by disease progression only in carotid artery plaques (381 proteins) with pathways as the nodes (node size corresponds to $-\log(q\text{-value})$) and shared detected proteins between pathways as the edges (edge thickness matches the Jaccard index of overlap between detected proteins of the two connected pathway nodes). Unbiased clustering of pathways into real network communities by the Louvain method revealed shared- and tissue-specific drivers of disease pathogenesis. Corresponds to Figure 2F.

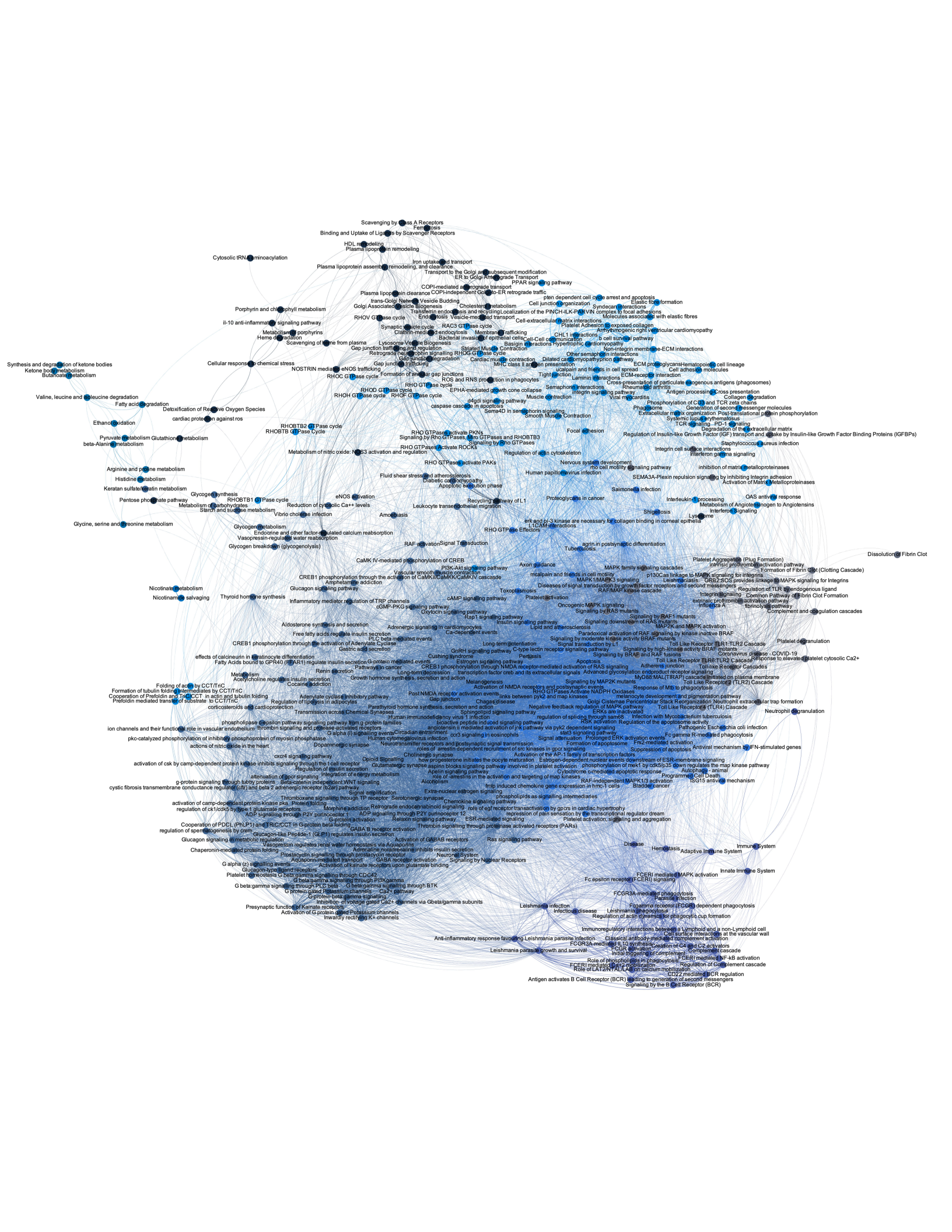
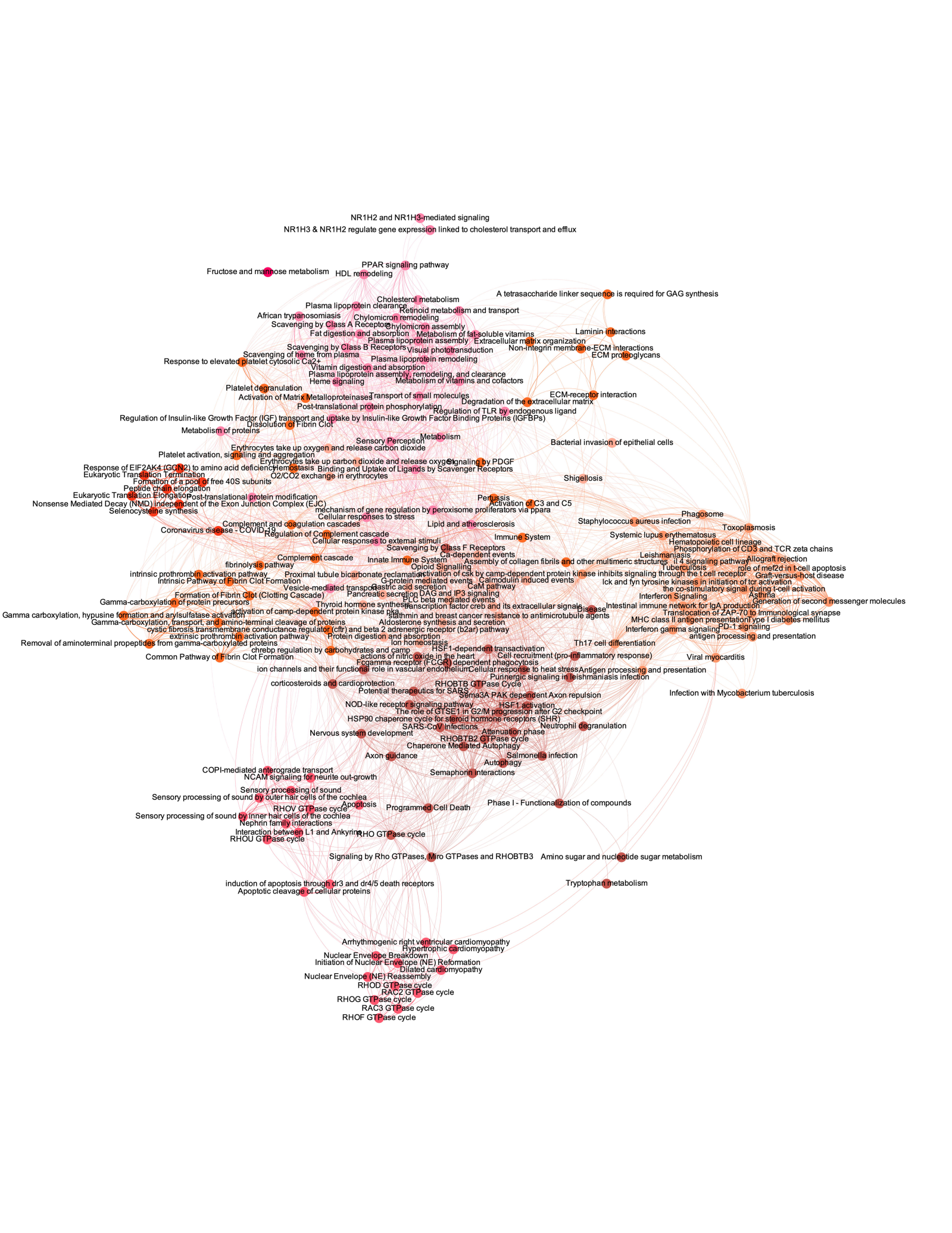


Figure S9: Labelled Network of Disease-Altered Pathways in Aortic Valve Whole Tissue.

Network based on KEGG, Reactome, and BioCarta pathway enrichment among proteins significantly differentially enriched by disease progression only in calcified aortic valves (226 proteins) with pathways as the nodes (node size corresponds to $-\log(q\text{-value})$) and shared detected proteins between pathways as the edges (edge thickness matches the Jaccard index of overlap between detected proteins of the two connected pathway nodes). Unbiased clustering of pathways into real network communities by the Louvain method revealed shared- and tissue-specific drivers of disease pathogenesis. Corresponds to Figure 2H.

Figure S10: Labelled Network of Disease-Altered Pathways in Carotid Artery and Aortic Valve Whole Tissue. Network based on KEGG, Reactome, and BioCarta pathway enrichment among proteins significantly differentially enriched by disease progression in both carotid artery plaques and calcified aortic valves (120 proteins) with pathways as the nodes (node size corresponds to $-\log(q\text{-value})$) and shared detected proteins between pathways as the edges (edge thickness matches the Jaccard index of overlap between detected proteins of the two connected pathway nodes). Unbiased clustering of pathways into real network communities by the Louvain method revealed shared- and tissue-specific drivers of disease pathogenesis. Corresponds to Figure 2G.



NR1H2 and NR1H3 mediated signaling
NR1H3 & NR1H2 regulate gene expression linked to cholesterol transport and efflux

Fructose and mannose metabolism HDL remodeling
PPAR signaling pathway

Cholesterol metabolism
A tetrasaccharide linker sequence is required for GAG synthesis

Plasma lipoprotein clearance
Retinoid metabolism and transport
Chylomicron remodeling
Chylomicron assembly

Scavenging by Class A Receptors
Laminin interactions
Fat digestion and absorption
Metabolism of fat-soluble vitamins
Extracellular matrix organization
Non-integrin membrane-ECM interactions
ECM proteoglycans

Response to elevated platelet cytosolic Ca²⁺
Scavenging of heme from plasma
Plasma lipoprotein remodeling
Vitamin digestion and absorption
Plasma lipoprotein assembly, remodeling, and clearance
Metabolism of vitamins and cofactors

Platelet degranulation
Metalloproteinase transport of small molecules
Degradation of the extracellular matrix
ECM-receptor interaction
Activation of Matrix Metalloproteinases
Post-translational protein phosphorylation
Regulation of TLR by endogenous ligand

Regulation of Insulin-like Growth Factor (IGF) transport and uptake by Insulin-like Growth Factor Binding Proteins (IGFBPs)
Dissolution of Fibrin Clot
Metabolism of proteins
Sensory Perception
Metabolism

Erythrocytes take up oxygen and release carbon dioxide
Platelet activation, signaling and aggregation
Erythrocytes take up carbon dioxide and release oxygen
Signaling by PDGF
Response of EIF2AK4 (GCN2) to amino acid deficiency
Hemostasis
Binding and Uptake of Ligands by Scavenger Receptors
Formation of a pool of free 40S subunits
O₂/CO₂ exchange in erythrocytes

Eukaryotic Translation Termination
Peptide chain elongation
Nonsense Mediated Decay (NMD) independent of the Exon Junction Complex (EJC)
Selenocysteine synthesis
Mechanism of gene regulation by peroxisome proliferators via ppara
Cellular responses to stress

Coronavirus disease - COVID-19
Complement and coagulation cascades
Lipid and atherosclerosis
Immune System
Regulation of Complement cascade
Cellular responses to external stimuli
Scavenging by Class F Receptors
Ca-dependent events

Innate Immune System
Opioid Signaling
Assembly of collagen fibrils and other multimeric structures
if 4 signaling pathway
fibrinolysis pathway
Proximal tubule bicarbonate reclamation
activation of csk by camp-dependent protein kinase inhibits signaling through the t cell receptor
Graft-versus-host disease
Intrinsic Pathway of Fibrin Clot Formation
Vesicle-mediated transcytosis
Calcium induced events
Calmodulin induced events
the co-stimulatory signal during t-cell activation

Formation of Fibrin Clot (Clotting Cascade)
Pancreatic secretion DAG and IP3 signaling
Calcium pathway
Gamma-carboxylation of protein precursors
Thyroid hormone synthesis
transcription factor creb and its extracellular signals
Intestinal immune network for IgA production
Generation of second messenger molecules

Gamma carboxylation, hypusine formation and arylsulfatase activation
activation of camp-dependent protein kinase
Sialmin and breast cancer resistance to antimicrotubule agents
Disase
Translocation of ZAP-70 to Immunological synapse
MHC class II antigen presentation
type I diabetes mellitus
Interferon gamma signaling
PD-1 signaling
antigen processing and presentation

Removal of aminoterminal propeptides from gamma-carboxylated proteins
extrinsic prothrombin activation pathway
Protein digestion and absorption
Ion homeostasis
Th17 cell differentiation
Virial myocarditis

Common Pathway of Fibrin Clot Formation
chrebp regulation by carbohydrates and camp
HSP1-dependent transactivation
actions of nitric oxide in the heart
Cell recruitment (pro-inflammatory response)
ion channels and their functional role in vascular endothelium
Cellular response to heat stress
Antigen processing and presentation
Purinergic signaling in leishmaniasis infection

corticosteroids and cardioprotection
RHOBTB2 GTPase Cycle
Sema3A PAK dependent Axon repulsion
Infection with Mycobacterium tuberculosis

NOD-like receptor signaling pathway
HSP1 activation
The role of G1 SE1 in G2M progression after G2 checkpoint
HSP90 chaperone cycle for steroid hormone receptors (SHR)
SARS-CoV Infections
Attenuation phase
Neutrophil degranulation

Nervous system development
RHOBTB2 GTPase cycle
Chaperone Mediated Autophagy
Autophagy
Salmonella infection

COPI-mediated anterograde transport
NCAM signaling for neurite out-growth
Sensory processing of sound
Apoptosis
Sensory processing of sound by outer hair cells of the cochlea
RHOV GTPase cycle
Programmed Cell Death
Phase I - Functionalization of compounds

Sensory processing of sound by inner hair cells of the cochlea
Nephrin family interactions
Interaction between L1 and Ankyrin
RHO GTPase cycle
Signaling by Rho GTPases, Micro GTPases and RHOBTB3
Amino sugar and nucleotide sugar metabolism

induction of apoptosis through dr3 and dr4/5 death receptors
Apoptotic cleavage of cellular proteins
Tryptophan metabolism

Arrhythmogenic right ventricular cardiomyopathy
Hypertrophic cardiomyopathy
Nuclear Envelope Breakdown
Initiation of Nuclear Envelope (NE) Reformation
Dilated cardiomyopathy
Nuclear Envelope (NE) Reassembly

RHOD GTPase cycle
RAC2 GTPase cycle
RHOG GTPase cycle
RAC3 GTPase cycle
RHOF GTPase cycle

Figure S11: OptiPrep Density Gradient Separation to Enrich Cardiovascular Tissue EVs.

A, Intact human carotid arteries were acquired from i) patients undergoing carotid endarterectomies due to carotid artery stenosis (diseased carotid artery atherosclerotic plaques) and ii) autopsy (normal carotid arteries). Intact human aortic valve (AV) leaflets were obtained from i) valve replacement surgeries due to AV stenosis (diseased calcified AVs), and ii) autopsy (normal AVs). Tissues promptly underwent rough dissection and enzymatic digestion with bacterial collagenase to dissociate the tissue components. Low-speed ultracentrifugation collected cells and debris, and the supernatant underwent high-speed centrifugation to pellet large microsomes and apoptotic bodies. The resultant supernatant was ultracentrifuged twice, with a wash step in between. The ultracentrifuged pellet (rich in EVs, as well as ECM, ribosomal debris, and protein aggregates) was overlaid on a linear 10-30% isosmotic iodixanol gradient, and OptiPrep density gradient separation was performed. **B,** In 15-fraction survey experiments ("EV Isolation Optimization"), each OptiPrep fraction was collected and pelleted separately by ultracentrifugation. Every fraction then underwent mass spectrometry, nanoparticle tracking analysis, and transmission electron microscopy. **C,** In EV-enriched OptiPrep fraction experiments ("Tissue EV Vesiculomics"), fractions 1-4 were pooled and pelleted together. High-resolution mass spectrometry, small RNA-seq, nanoparticle tracking analysis, and electron microscopy were completed on the pooled EV-enriched fractions.

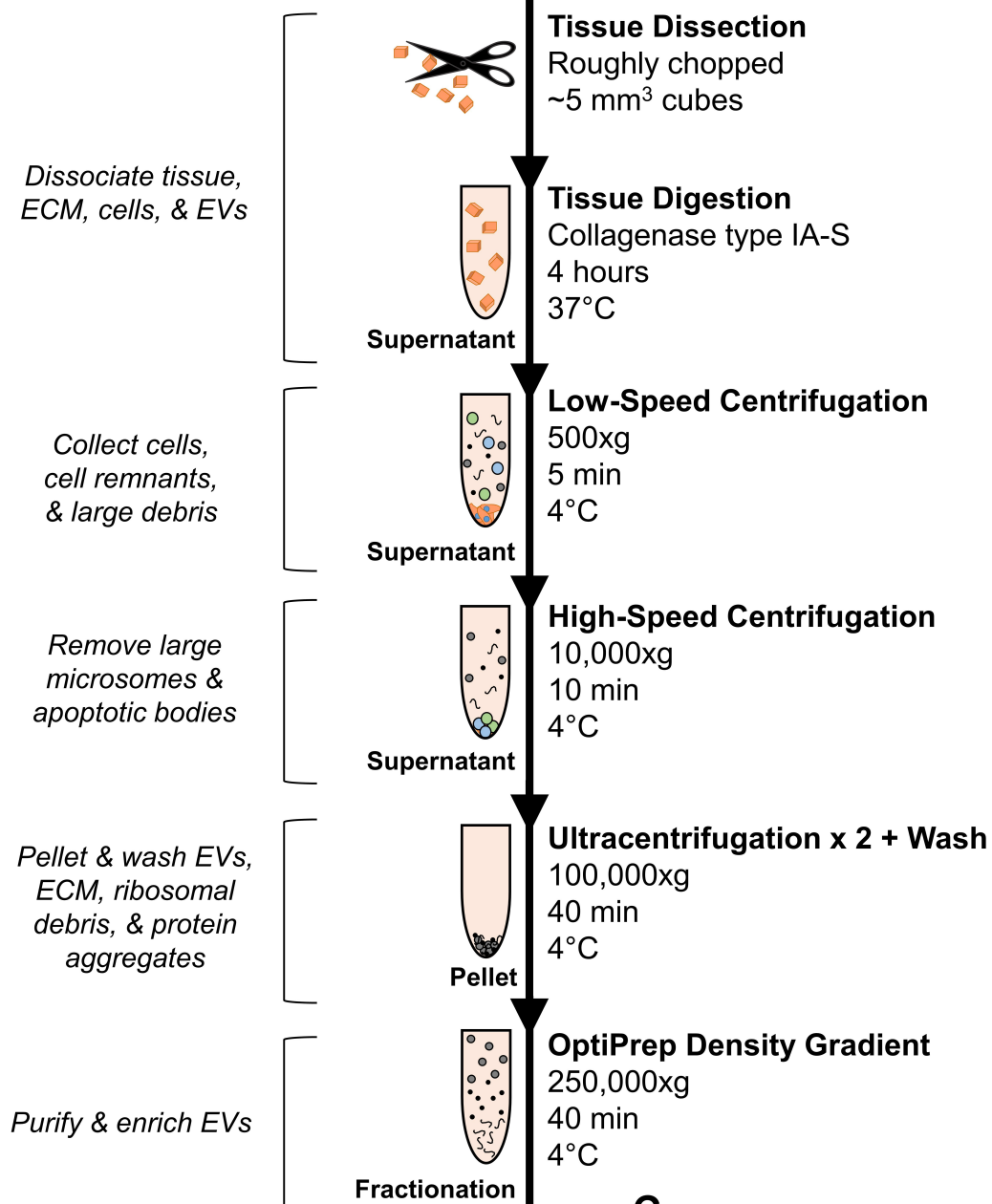
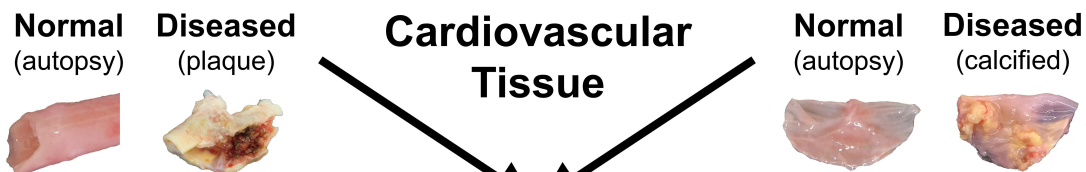
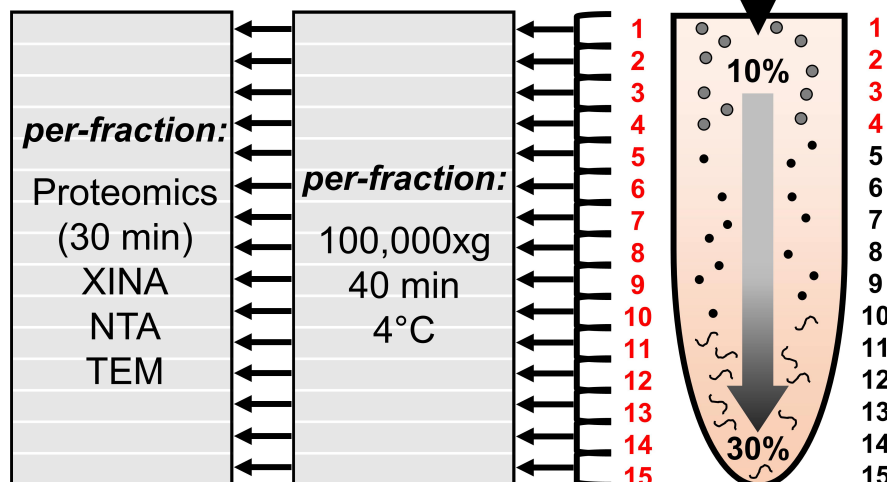
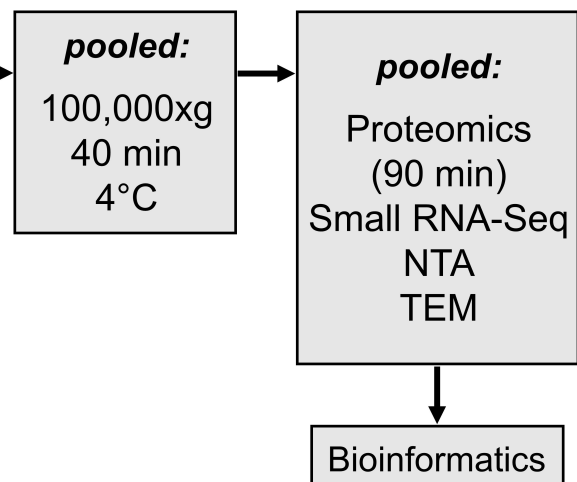
A**Carotid Artery****Aortic Valve****B****15-Fraction Surveys****C****EV-Enriched OptiPrep Fractions**

Figure S12: EV Enrichment by OptiPrep Separation – EV Markers and XINA Co-abundance Profiling. **A**, From 15-fraction survey experiments (“EV Isolation Optimization”) on intact human carotid artery plaques (left) and calcified aortic valves (right), protein abundance heat maps of 22 EV markers across 15 OptiPrep density gradient fractions found that EV marker proteins were consistently enriched in the four least-dense fractions of both tissue types; n=3 carotid artery plaque and 4 aortic valve donors. **B**, Tissue-specific XINA coabundance profiling of protein abundances in OptiPrep fractions 1-4 from atherosclerotic plaques (left) and calcified aortic valves (right). Proteins detected in the 5 clusters per tissue type whose protein abundance profiles mimicked those of the 22 EV markers in part A (elevated in fractions 2 and 3; brown clusters 1, 2, 5, 6, 9 and 1, 5, 6, 8, 10 for atherosclerotic plaque and aortic valve, respectively) were subjected to gene ontology analysis. Highly significant GO terms in these clusters were largely associated with vesicular processes and further demonstrated EV enrichment in the least-dense OptiPrep fractions.

OptiPrep Fractionation – MS/MS

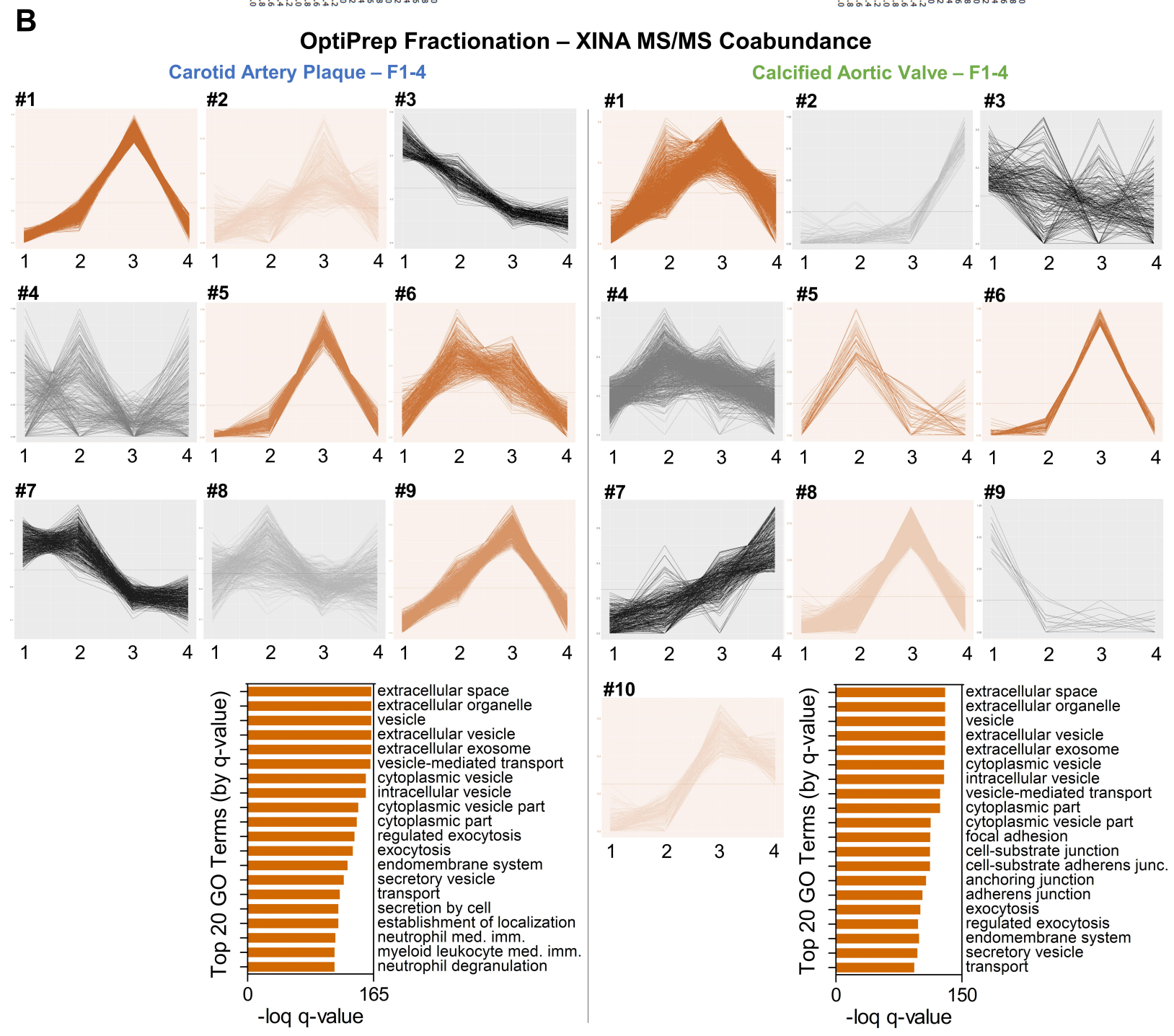
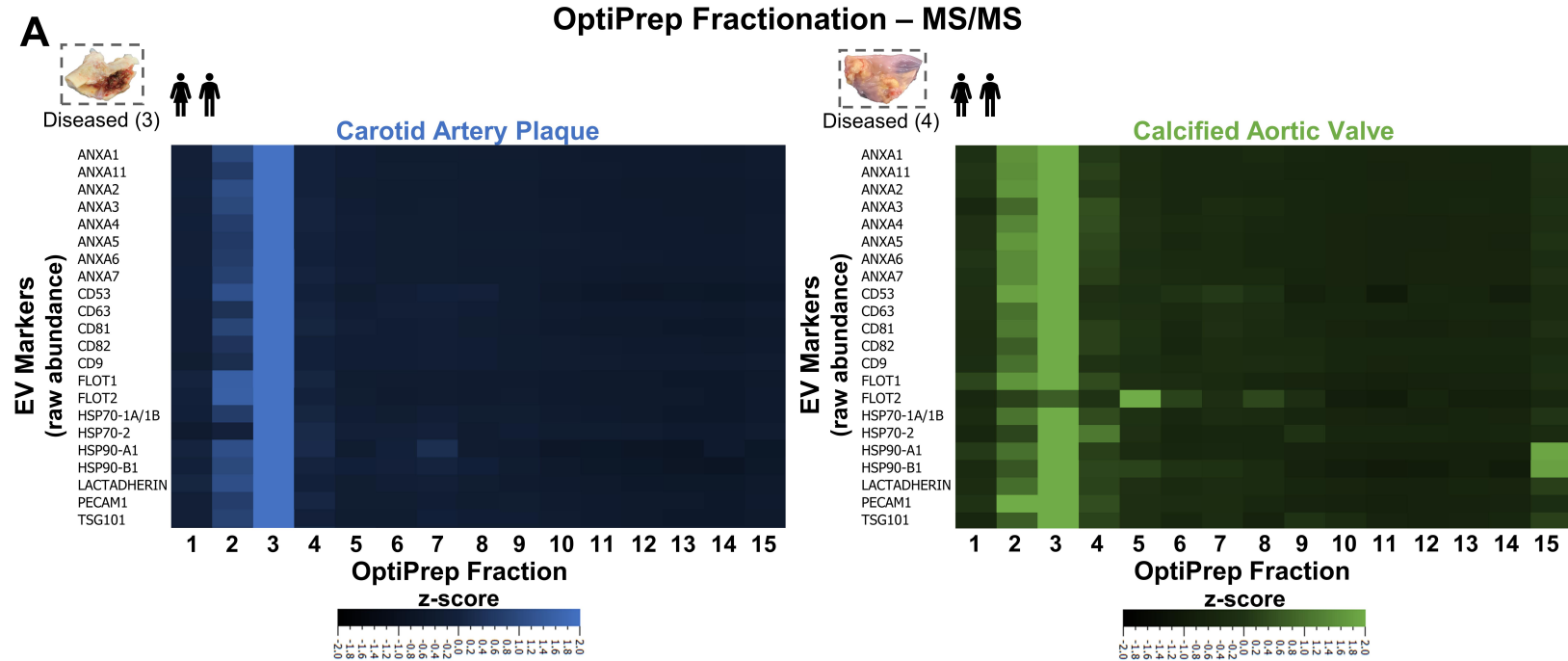


Figure S13: Transmission Electron Microscopy of 15-Fraction Survey Experiments. A and B, Representative CD63-labelled immunogold transmission electron microscopy (TEM) and negative controls from OptiPrep fractions 1-15 of human carotid artery plaques (A) and calcified aortic valves (B) demonstrated fraction density-dependent enrichment of extracellular vesicles, globular collagen, and fibrillar collagen.

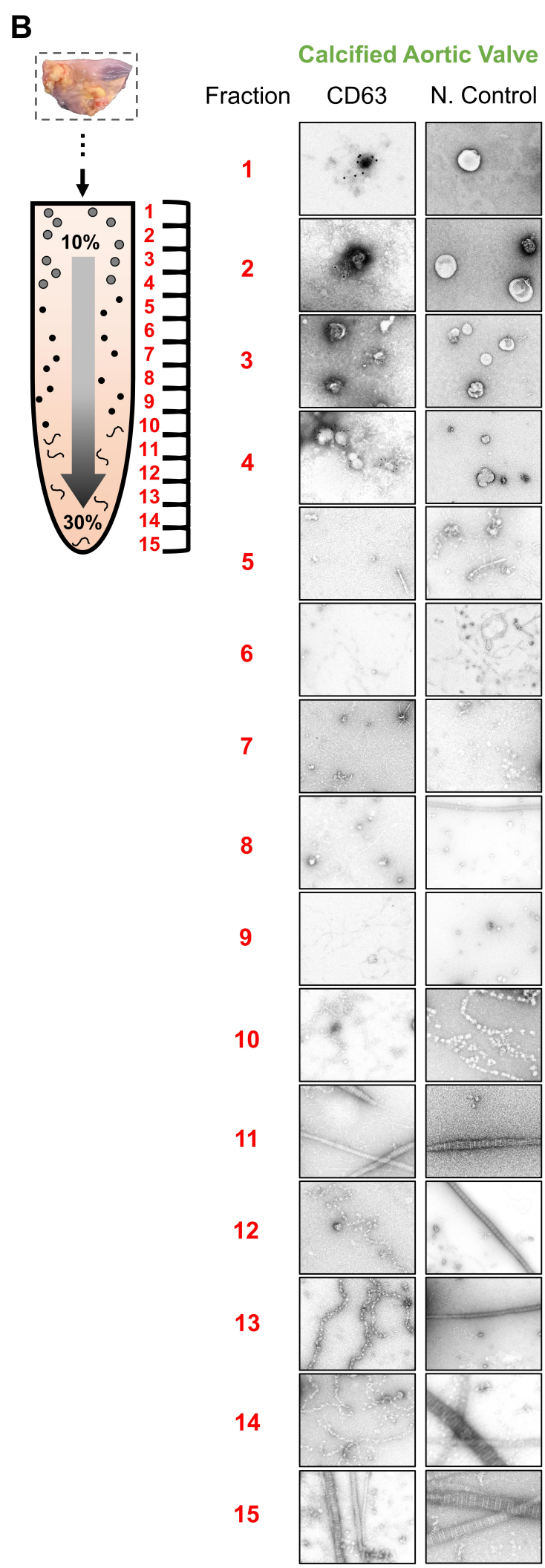
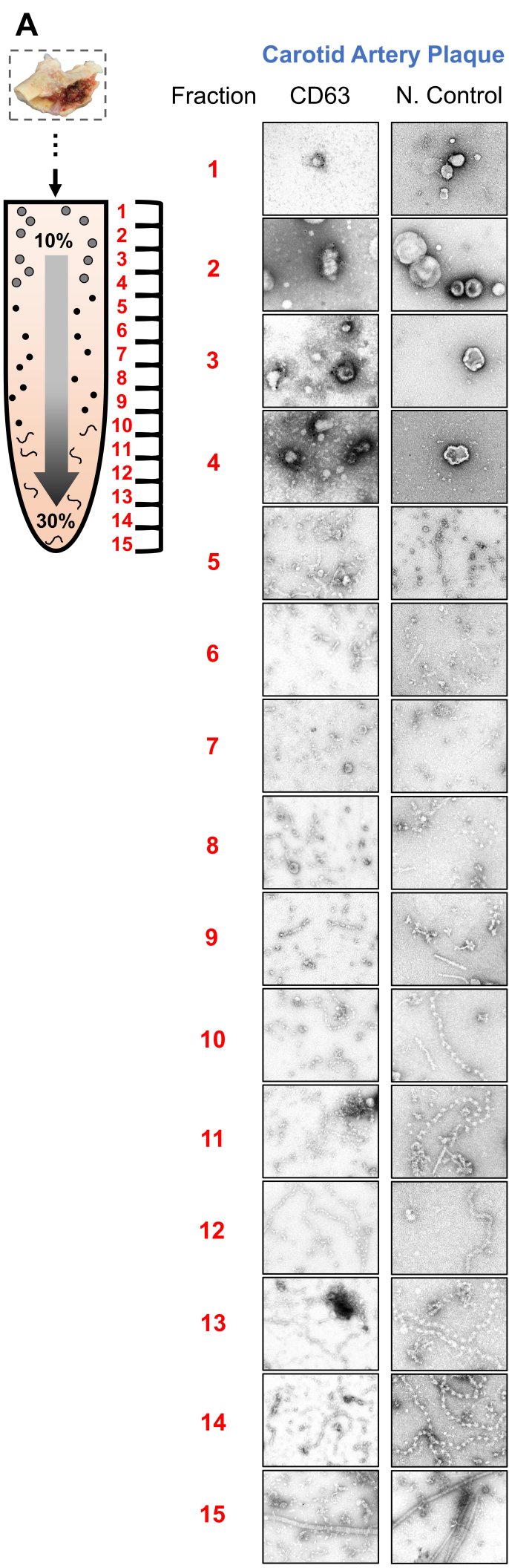


Figure S14: Transmission Electron Microscopy Negative Controls. Representative negative control transmission electron microscopy (corresponding to Figure 3C) identified membrane-bound EVs in OptiPrep fractions 1-4 (arrows) from carotid artery plaques (top) and calcified aortic valves (bottom); bar=100 nm. Consistent with mass spectrometry-derived protein abundance, TEM showed abundant globular collagens in fractions 5-10 (arrowheads) and fibrillar collagens in the most-dense fractions (open arrows).

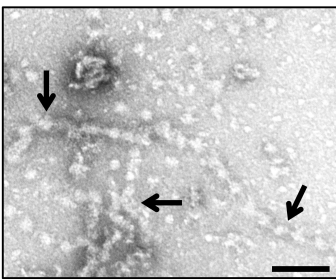
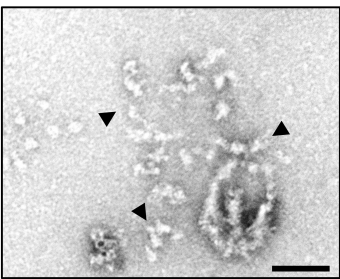
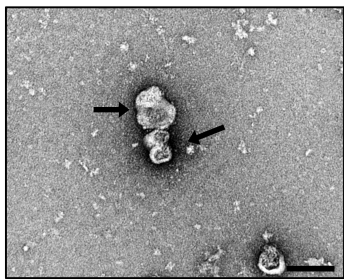
Negative Control

F1-4

F5-10

F11-15

Carotid Artery
Plaque



Calcified
Aortic Valve

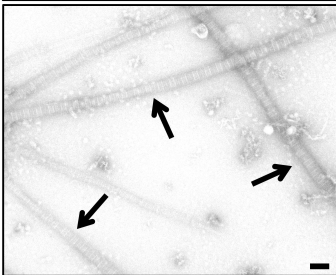
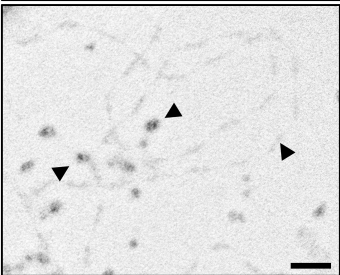
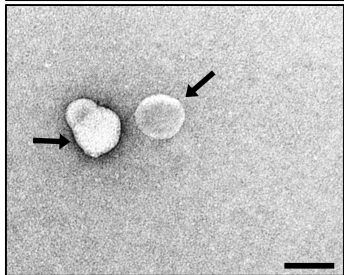


Figure S15: Tissue EVs Purified by Ultracentrifugation Alone Show Marked Extracellular

Matrix Contamination. A, Purification of extracellular vesicles (EVs) was assessed by comparing the proteome collected by ultracentrifugation alone vs. EVs enriched by pooling fractions 1-4 of an OptiPrep density gradient. **B,** Proteomics found that the OptiPrep-derived EV proteome was >38% deeper than that of EVs obtained by ultracentrifugation alone in both carotid artery plaque (n=3; 39.7% larger) and calcified aortic valve tissues (n=4; 38.1% larger). **C,** Top 10 gene ontology (cellular component) and UniProt keyword analyses of those proteins unique to ultracentrifugation found an abundance of extracellular matrix and endoplasmic reticulum protein contaminants when tissue-derived EVs were extracted by ultracentrifugation alone. Meanwhile, OptiPrep enrichment enabled detection of additional intracellular-, membrane- and vesicle-associated proteins linked with diverse biological functions (e.g. phosphorylation, protein transport, post-translational modification, actin-binding, etc.).

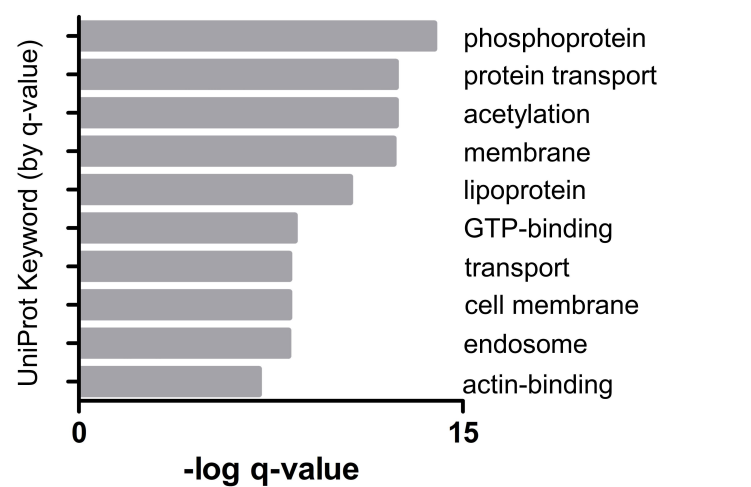
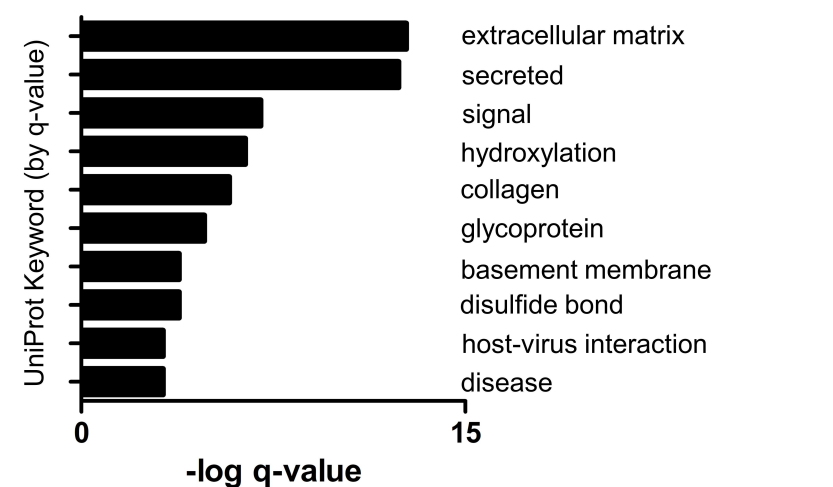
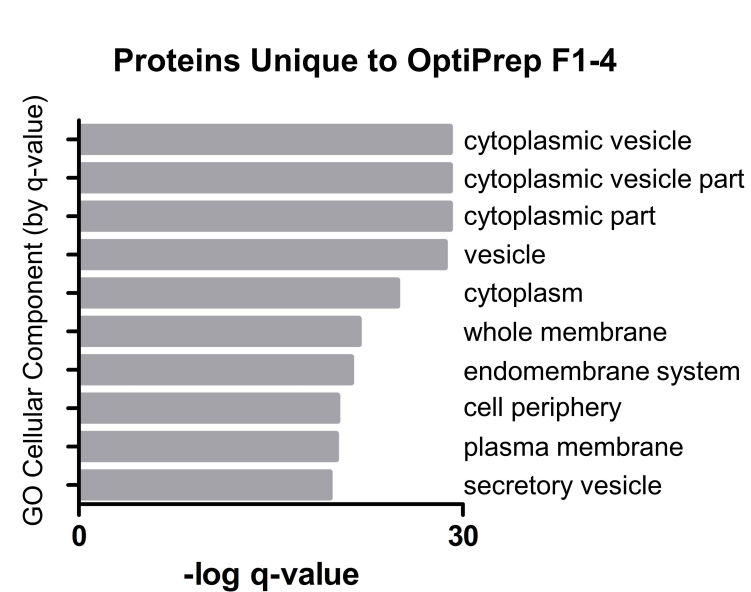
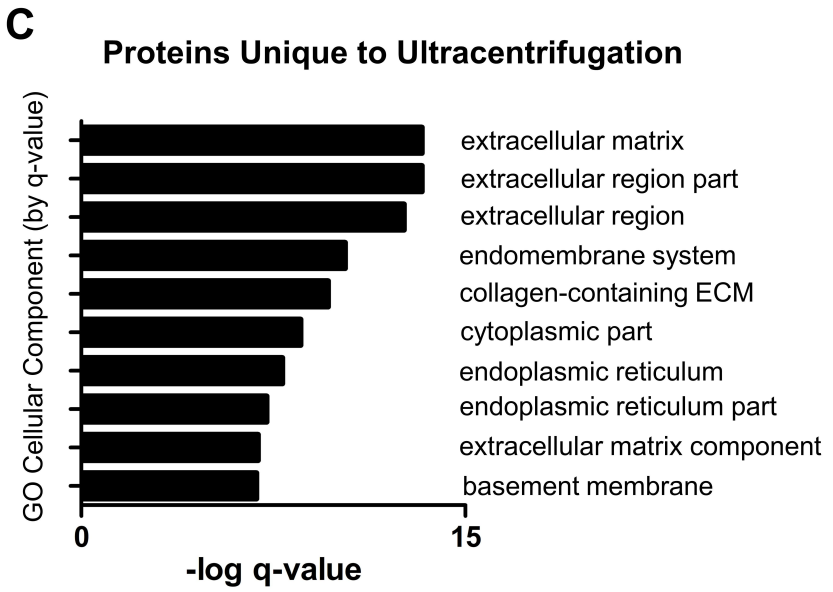
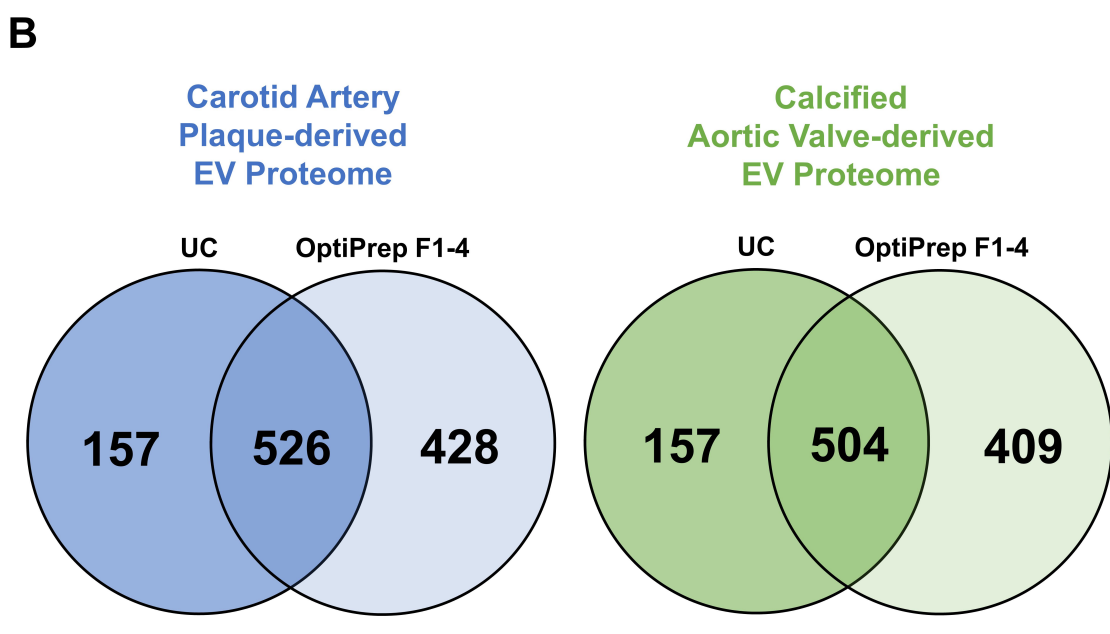
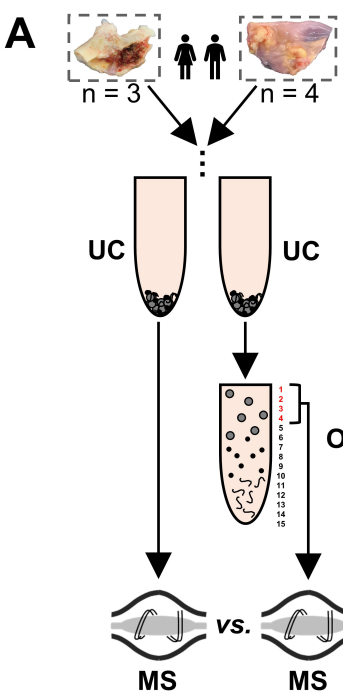


Figure S16: Elimination of Iodixanol From Mass Spectrometry by Targeted Mass

Exclusion Windows. A, Total ion current spiked during mass spectrometry of samples prepared by OptiPrep density gradient (gold shading: representative spiking at 28-34 minutes during a 90-minute gradient). **B,** MS scans from 28-34 minutes of a 90-minute gradient, showing a highly-abundant precursor ion (775.86354, $z=2$, purple shading) consistent with carryover of iodixanol contamination from the OptiPrep gradient (theoretical mass=1549.7133 u). **C,** The 775.8 m/z precursor eluted repeatedly between 28-34 minutes; inset: peaks in the range of ~775.8 m/z were limited to this RT window. **D,** Despite dynamic exclusion of identical precursor ions, peptide sequencing events were frequently performed on fragment ions from the 775.86354 m/z iodixanol contaminant. **E,** Flow chart describing the peptide sequencing approach that was subsequently employed to avoid wasting sequencing events on iodixanol precursor ions. Targeted mass exclusion was enacted at an m/z of 775.8645 ($z=2$), an exclusion mass width of 10 ppm, over a 4 minute (30-minute gradients) or 7-minute (90-minute gradients) retention time window. **F,** The total number of proteins detected increased by 9.5% with targeted mass exclusion of EV-enriched pooled fractions from 4 intact carotid artery plaque and 4 intact calcified aortic valve donors (955 vs. 1,046 proteins). The 198 proteins unique to targeted mass exclusion comprised a tightly associated protein-protein interaction network and 20 significantly enriched KEGG pathways, while those lost during targeted exclusion had no significant pathway enrichment.

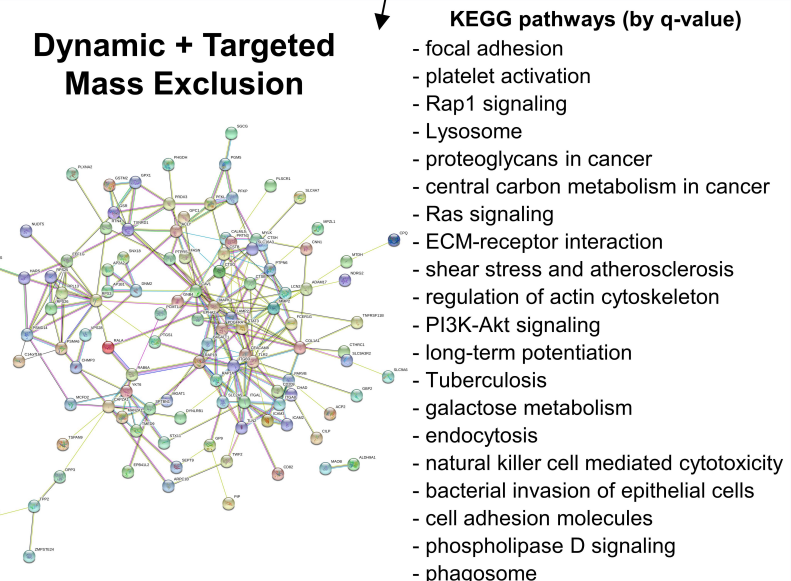
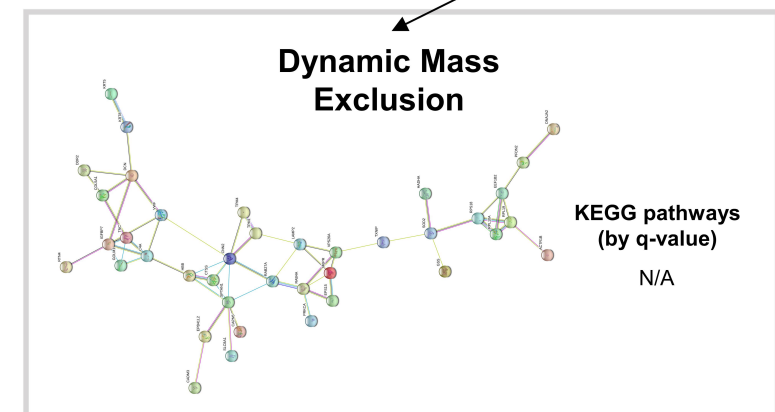
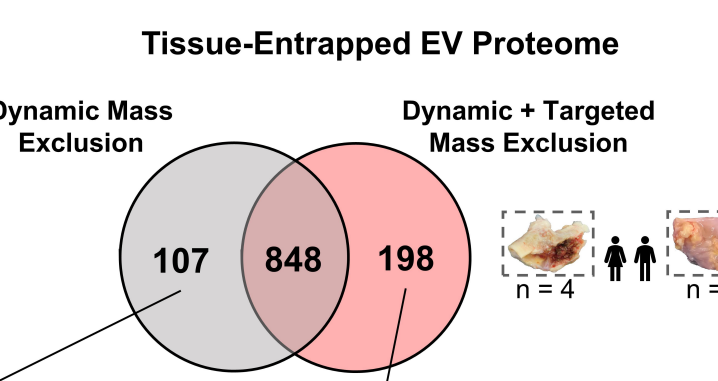
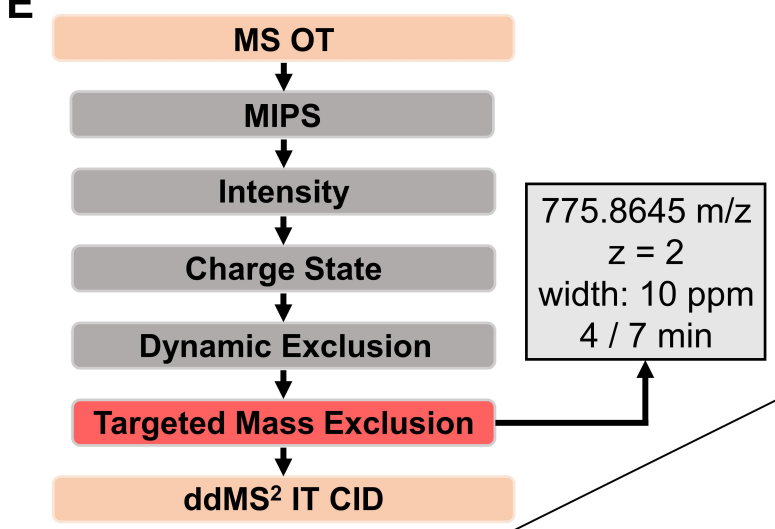
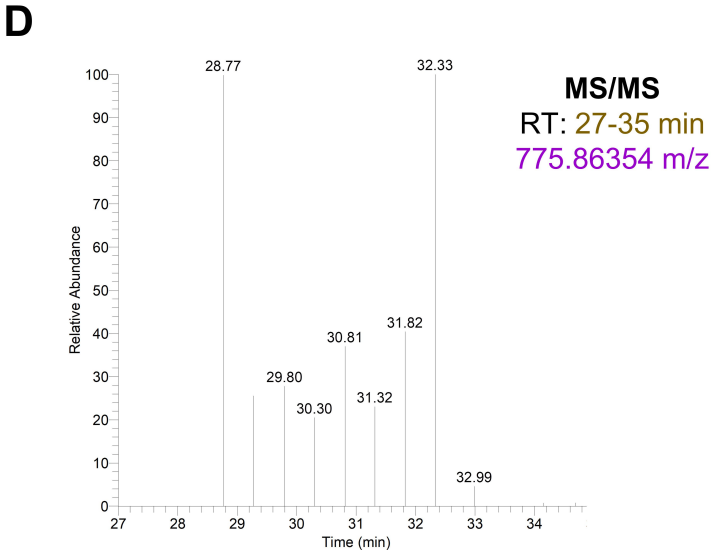
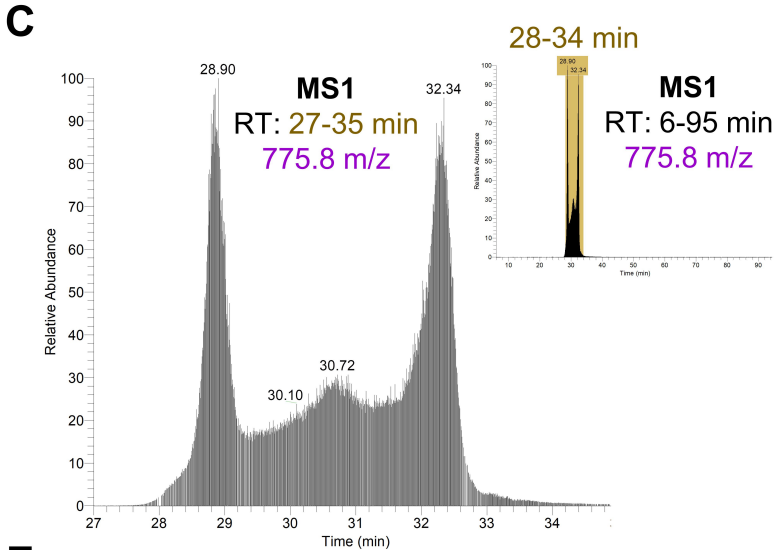
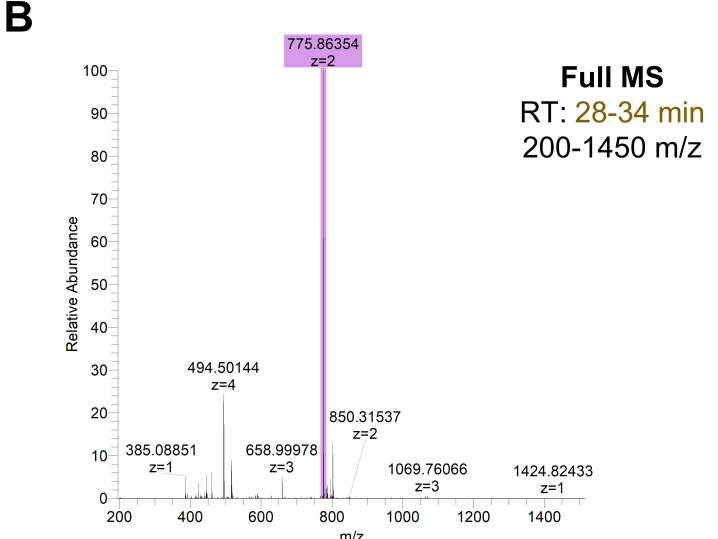
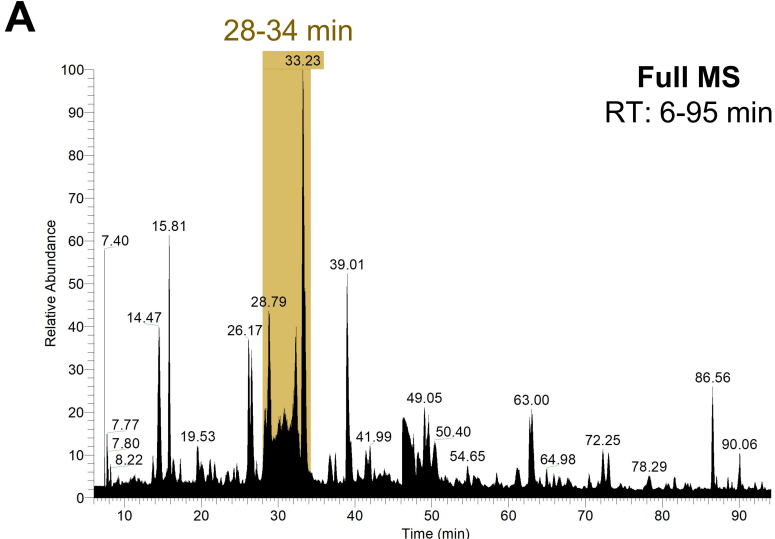


Figure S17: Mock Iodixanol-Only OptiPrep Fractions. **A**, Mock OptiPrep fractions prepared in the absence of ultracentrifuged tissue digest (i.e. containing only iodixanol and NTE buffer) continued to demonstrate spikes in full MS total ion current (gold shading: representative spiking at 17-21 minutes during a 30-minute gradient). **B**, The 775.86343 m/z precursor ion (purple shading) continued to be highly abundant during this retention time window. **C**, Peaks in the range of ~775 m/z were limited to this time period. Together, this data indicated that these peaks were not biological peptides derived from cardiovascular tissue, but rather residual iodixanol contamination.

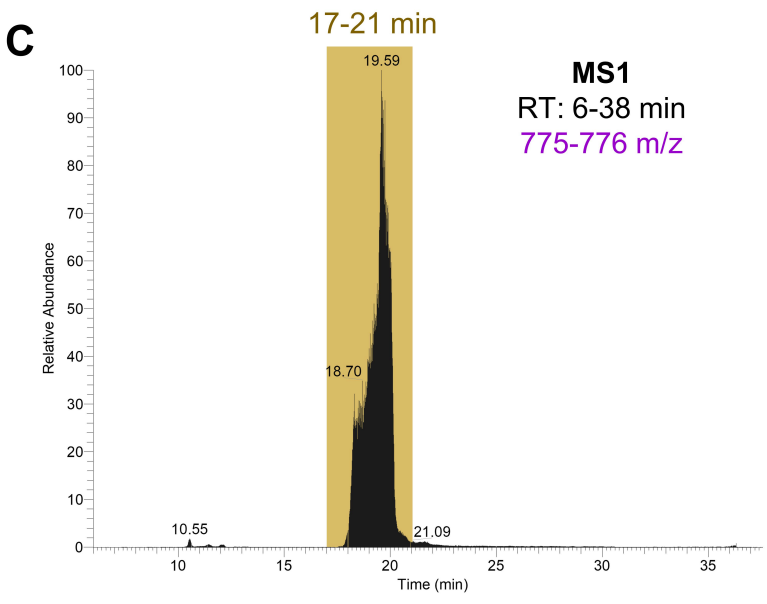
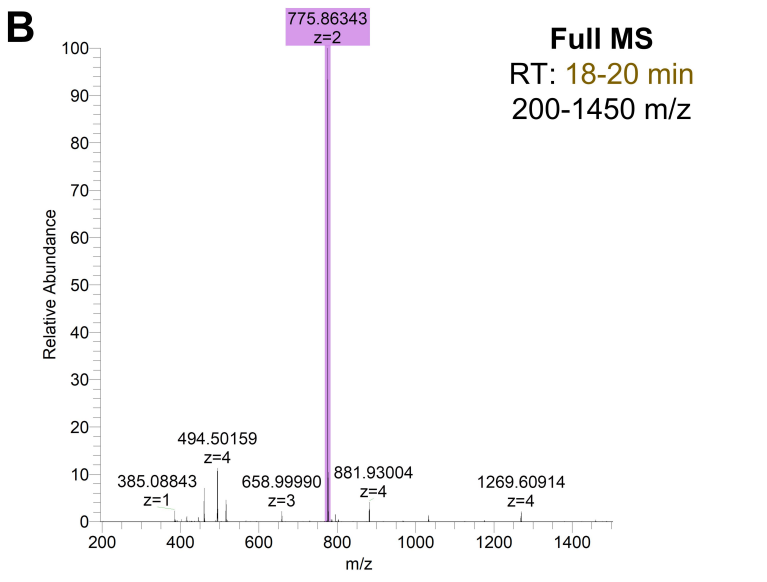
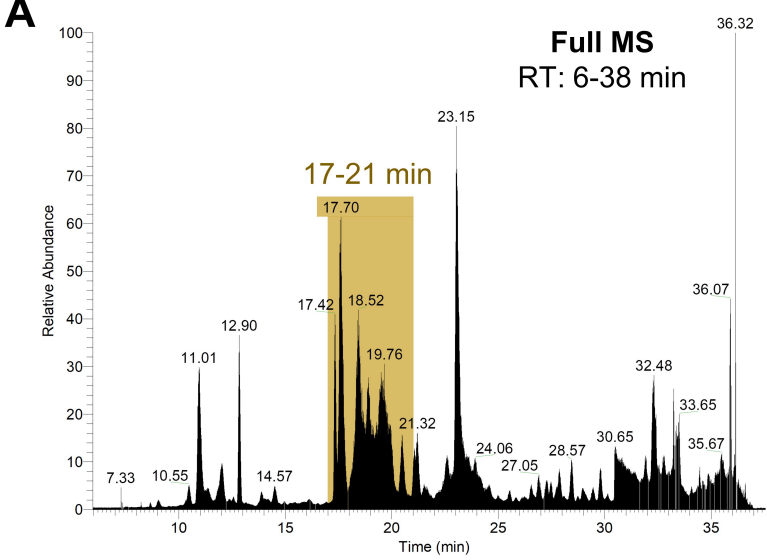


Figure S18: Histology of Normal and Diseased Tissues. A and B, Representative histological staining of normal (autopsy) and diseased carotid artery cross-sections (from carotid endarterectomy due to carotid artery stenosis) and aortic valve longitudinal (tip-to-base) sections (from aortic valve replacement due to aortic valve stenosis) by hematoxylin and eosin for morphology and pathology (**A**, H&E) and von Kossa (**B**) for calcification. All scale bars = 200 μ m. L = lumen, F = fibrosa, V = ventricularis. **C**, Quantitative histopathological score indices (0-3, none/mild/moderate/severe; summed for overall disease) for inflammation, fibrosis, calcification, and overall disease of 3 sections per stain per donor demonstrated i) minimal histological markers of disease in normal tissues, ii) significant increases in histological disease burden between normal and diseased tissues, and iii) no significant differences in histological disease burden between carotid artery and aortic valve tissue types. Box plots 25th-75th percentiles; line = median; “+” = mean; whiskers represent minimum and maximum values; n=4-6 donors per group; ***p<0.001, ****p<0.0001.

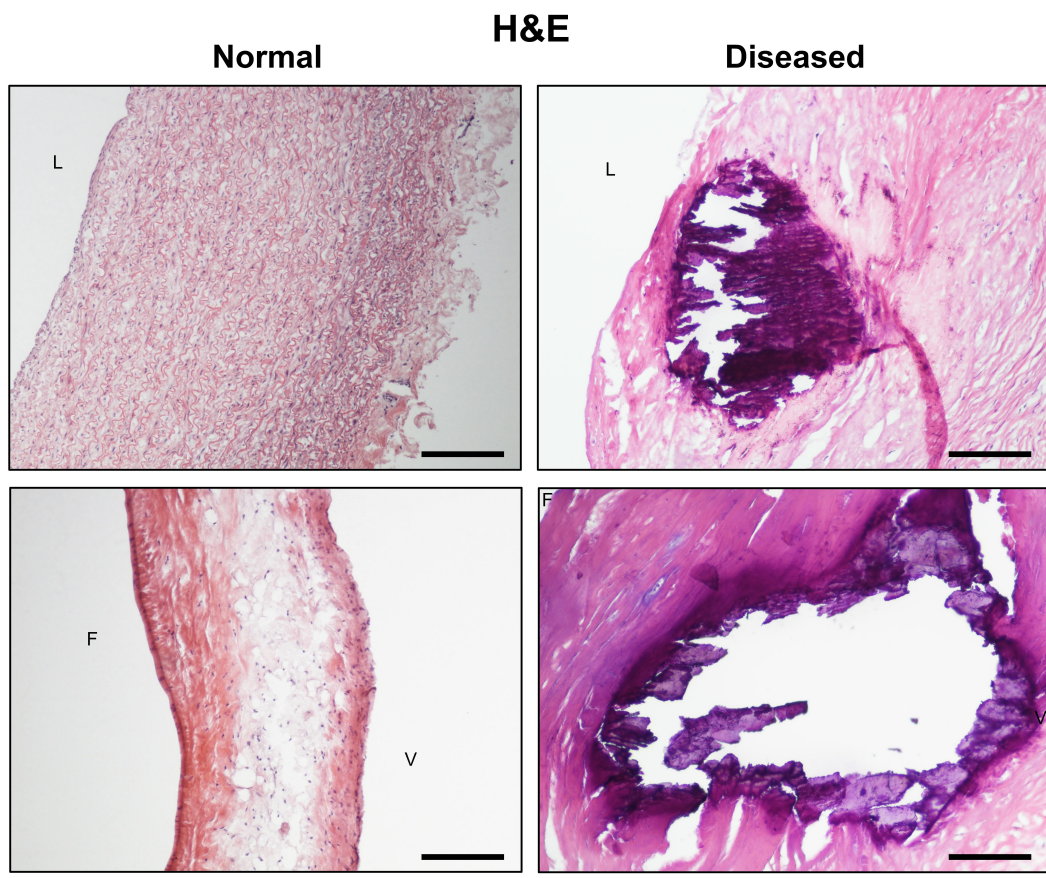
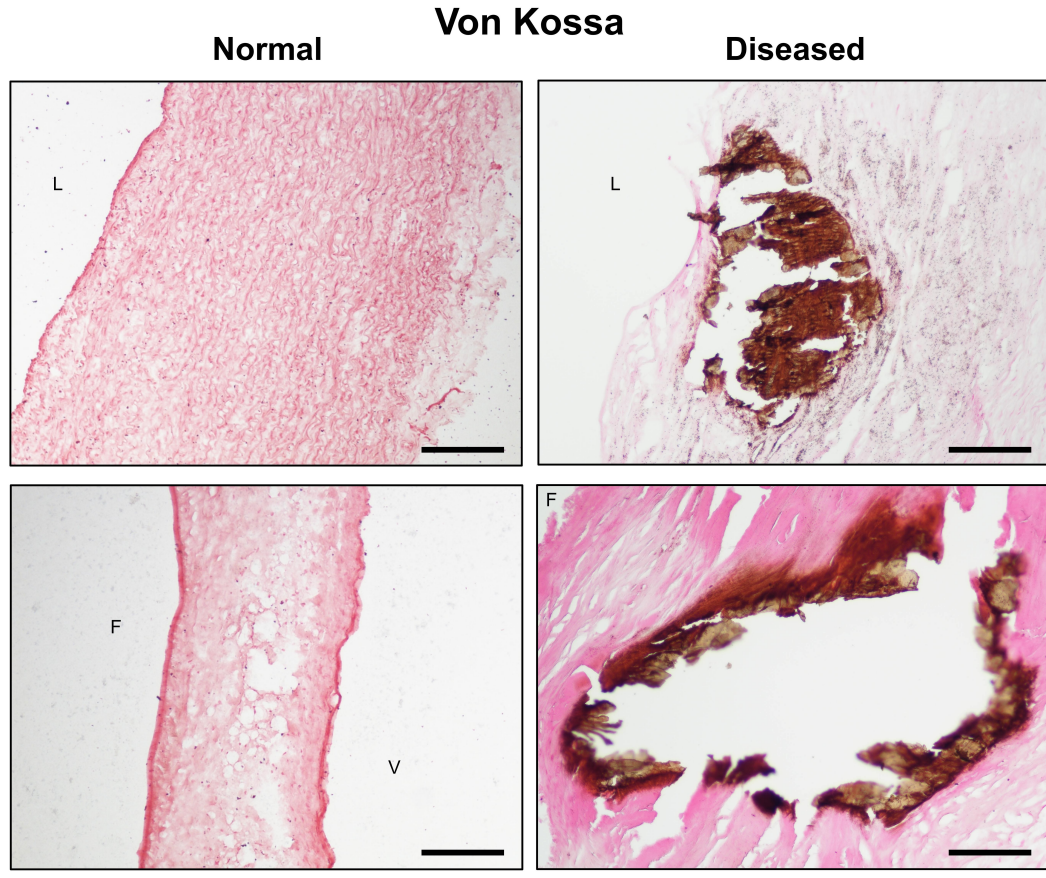
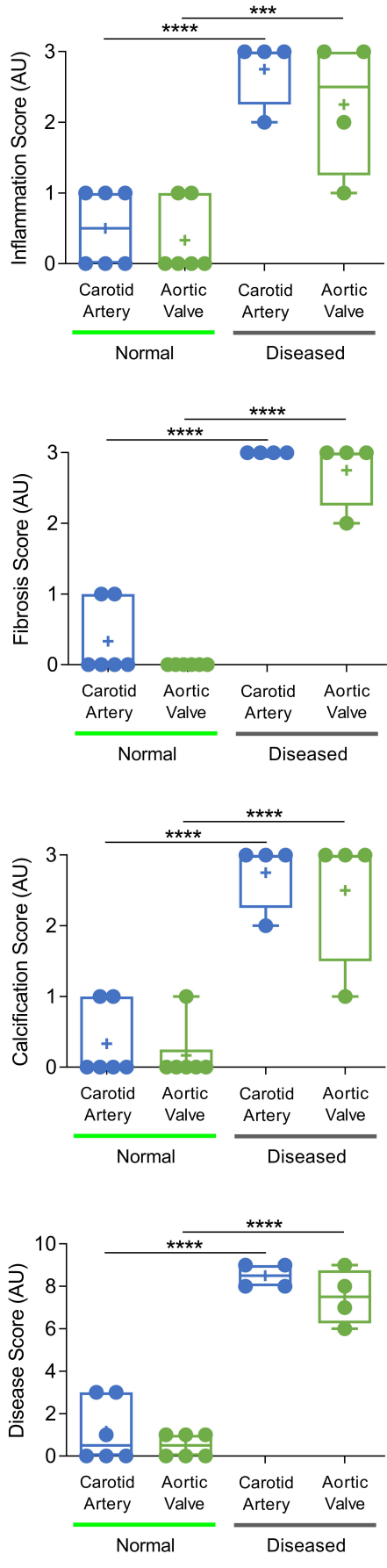
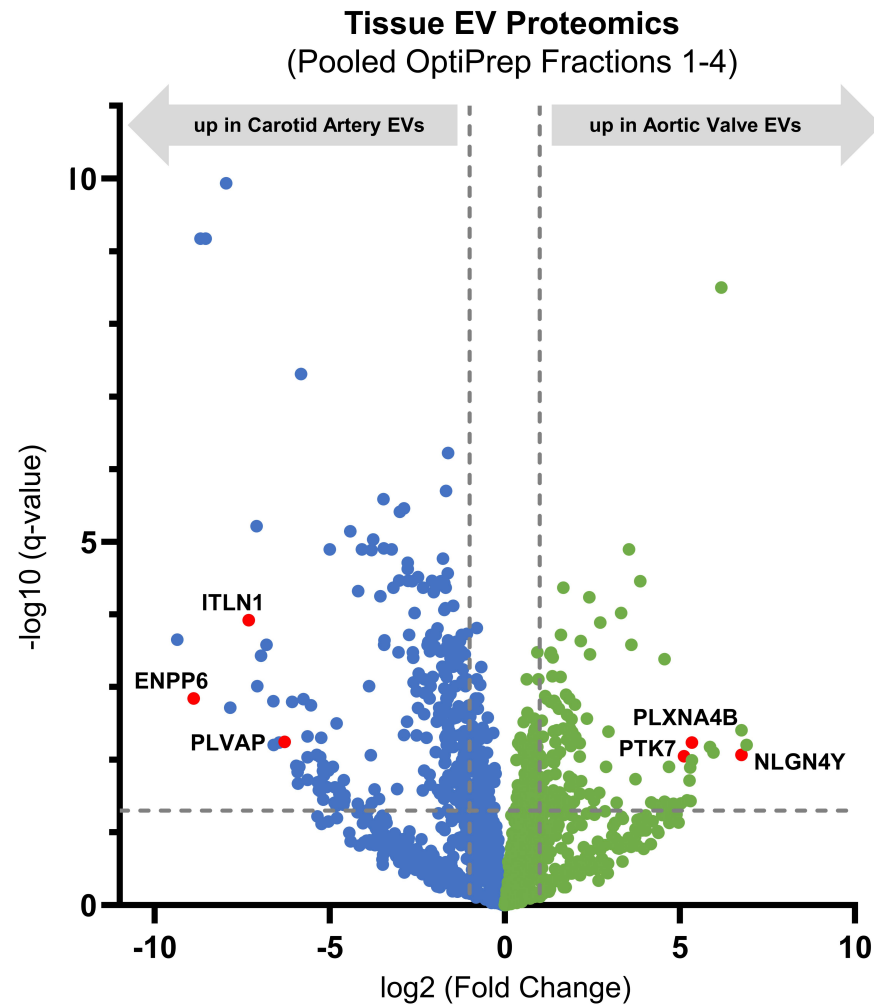
A**Carotid Artery****Aortic Valve****B****Carotid Artery****Aortic Valve****C**

Figure S19: Proteomics and Immunogold-TEM of Tissue EVs. **A**, Volcano plot of 1,942 proteins quantified by label-free proteomics of tissue EVs isolated via pooled OptiPrep fractions 1-4 from intact human carotid arteries (n=6) and aortic valves (n=6) identified components of the tissue EV proteome including ITLN1, ENPP6, PLVAP (up in carotid artery EVs) and PLXNA4B, PTK7, NLGN4Y (up in aortic valve EVs) that were highly and significantly differentially enriched; cutoffs at a fold-change of 2 and a q-value of 0.05. **B**, Representative ITLN1, ENPP6, PLVAP, PLXNA4B, PTK7, and NLGN4Y-labelled immunogold transmission electron microscopy (TEM) images from pooled OptiPrep fractions 1-4 of human carotid artery (left) and aortic valve (right) demonstrated tissue-specific EV cargo enrichment in strong accordance with proteomics findings; bar=100 nm.

A**B**

Immunogold Transmission Electron Microscopy
(Pooled OptiPrep Fractions 1-4)

Carotid Artery EVs

Aortic Valve EVs

Carotid Artery EVs

Aortic Valve EVs

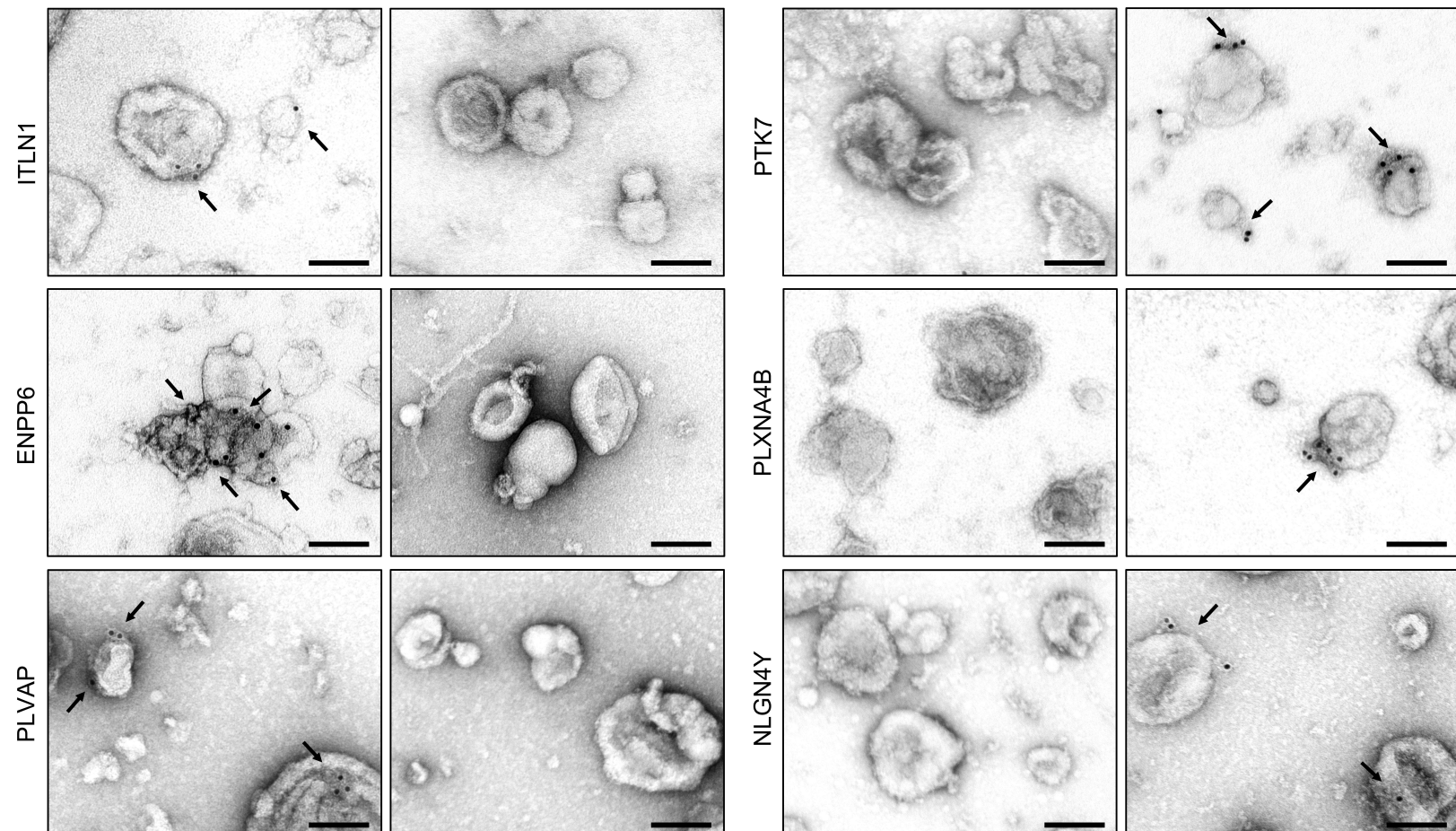
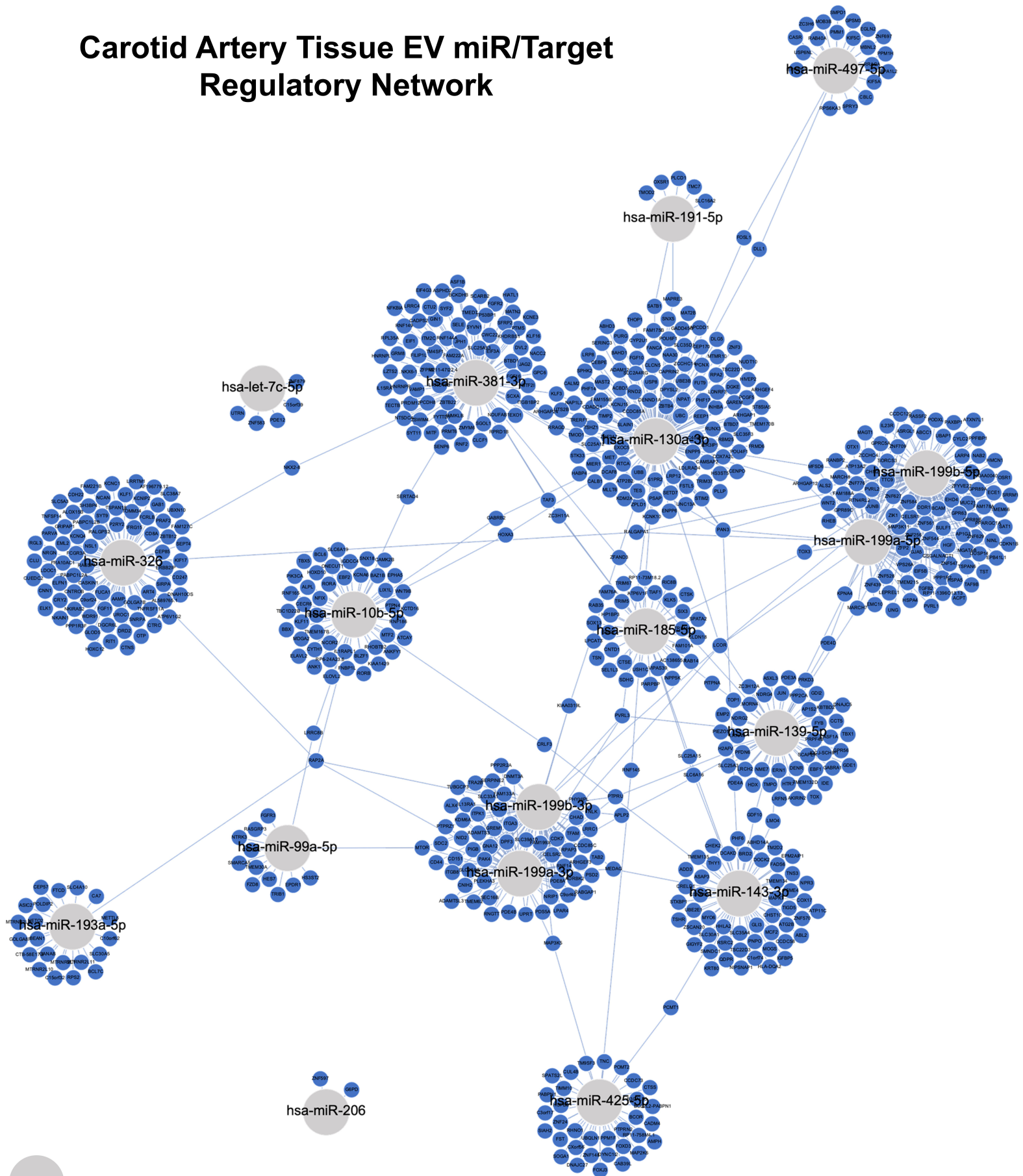


Figure S20: Labelled miR/Target Regulatory Network of miRs and Unique Gene Targets Changed by Disease Only in Carotid Tissue EVs. miR/target regulatory network of TargetScan-predicted gene targets ($\geq 95^{\text{th}}$ percentile weighted context++ score) of tissue EV miRs altered by disease progression only in carotid arteries. Corresponds to Figure 5C.

Carotid Artery Tissue EV miR/Target Regulatory Network





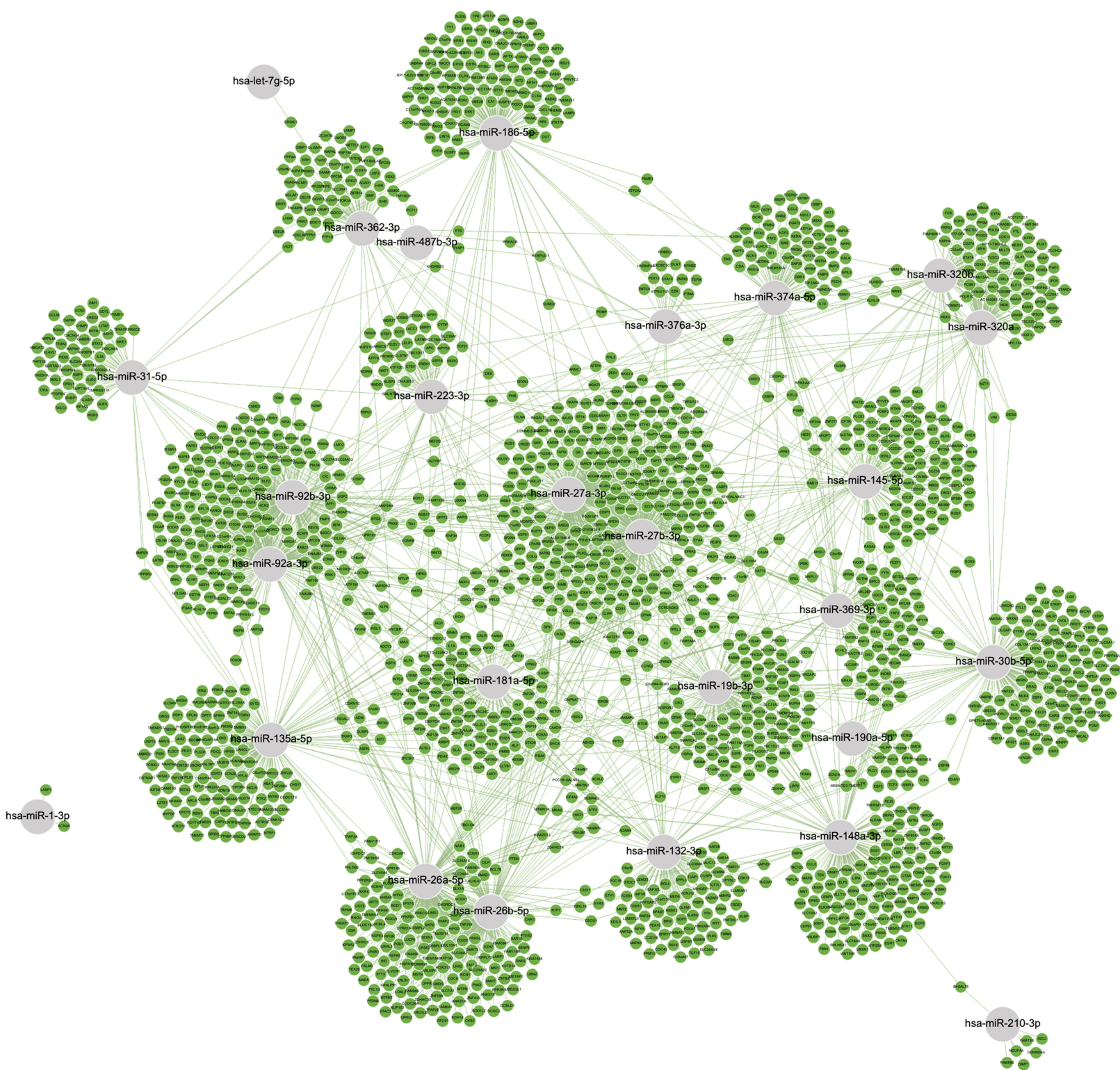
-  Enriched Tissue EV miRNAs
-  mRNA Targets of Enriched Tissue EV miRNAs

Figure S21: Labelled miR/Target Regulatory Network of miRs and Unique Gene Targets Changed by Disease in Carotid and Aortic Valve Tissue EVs. miR/target regulatory networks of TargetScan-predicted gene targets ($\geq 95^{\text{th}}$ percentile weighted context++ score) of tissue EV miRs altered by disease progression in both carotid arteries and aortic valves. Corresponds to Figure 5C.

Figure S22: Labelled miR/Target Regulatory Network of miRs and Unique Gene Targets Changed by Disease Only in Aortic Valve Tissue EVs. miR/target regulatory networks of TargetScan-predicted gene targets ($\geq 95^{\text{th}}$ percentile weighted context++ score) of tissue EV miRs altered by disease progression only in aortic valves. Corresponds to Figure 5C.

Aortic Valve Tissue EV miR/Target Regulatory Network



- Enriched Tissue EV miRNAs
- mRNA Targets of Enriched Tissue EV miRNAs

Figure S23: Labelled Integrated Network of Disease-Altered Proteomics and Transcriptomic Pathways Shared in Tissue EVs. The network of 50 overlapping KEGG, Reactome, and BioCarta pathways that were significantly enriched in the proteome and gene targets of miRs altered by disease in both carotid artery and aortic valve tissue EVs (n=6 normal carotid arteries, n=4 diseased carotid artery atherosclerotic plaques, n=6 normal aortic valves, n=4 diseased calcified aortic valves). Pathways are nodes (node size corresponds to $-\log(q\text{-value})$) and shared detected genes between pathways are edges (edge thickness matches the Jaccard index of overlap between detected genes of the two connected pathway nodes). Louvain clustering revealed 4 distinct annotations shared by disease-altered cardiovascular tissue-derived EV cargoes, including cell cycle regulation and apoptosis, synthesis and organization of the extracellular matrix (ECM), and modulation of intracellular signaling cascades. Corresponds to Figure 6A/B.

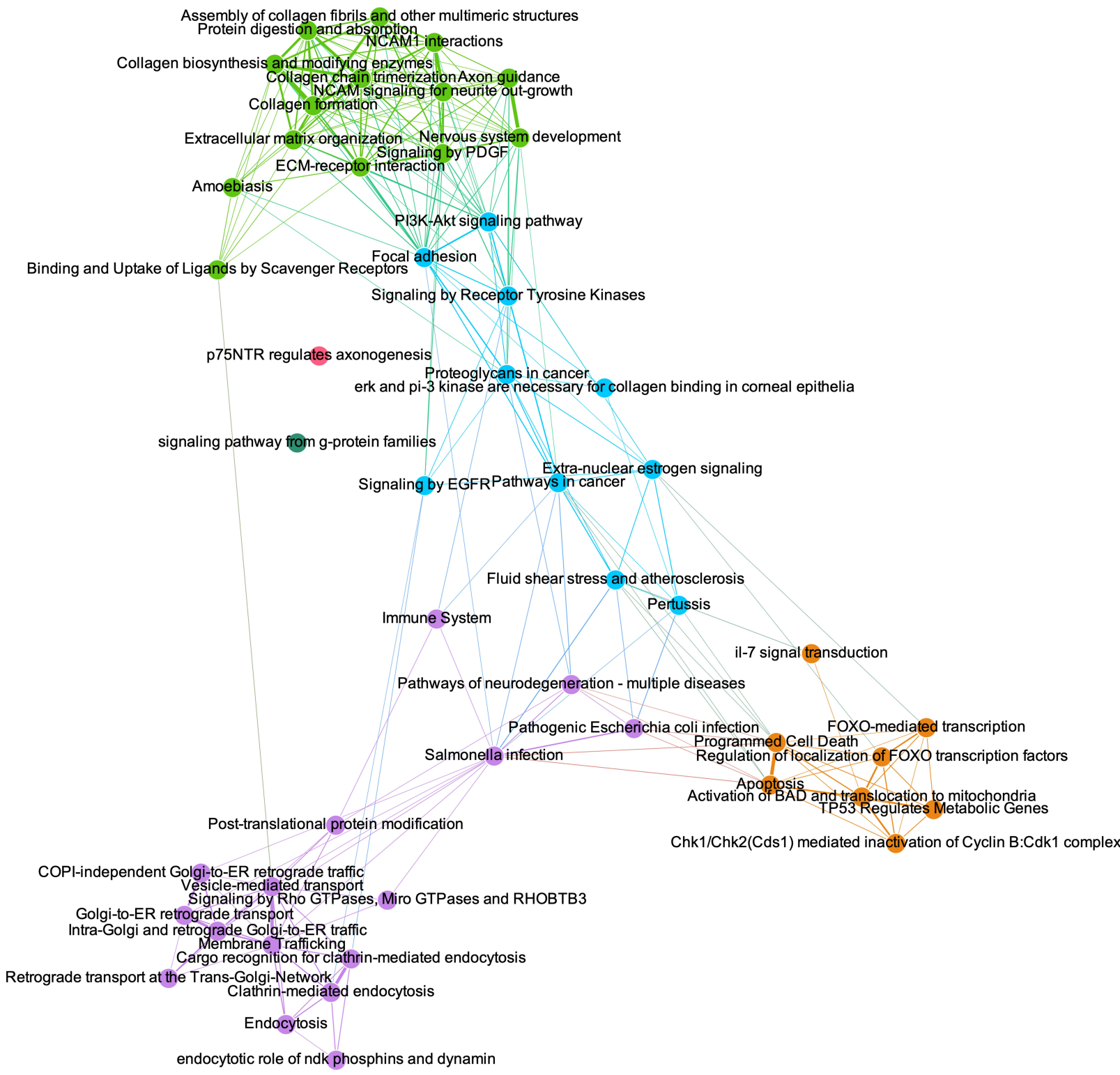


Figure S24: Reciprocal Knockdown Experiments of EV-derived Targets in hCtASMCs and hVICs. **A and C**, Relative mRNA expression levels of *WNT5A*, *APP*, *APC*, *FGFR2*, *PPP2CA*, and *ADAM17* vs. *GAPDH* in primary human carotid artery smooth muscle cells (hCtASMCs, **A**) and human aortic valvular interstitial cells (hVICs, **C**) after 6 days in normal medium (NM) incubated with scrambled siRNA (siSCR) or siRNA targeting *WNT5A*, *APP*, *APC*, *FGFR2*, *PPP2CA*, or *ADAM17* (siWNT5A, siAPP, siAPC, siFGFR2, siPPP2CA, siADAM17) demonstrated robust knockdown of target gene expression; n=1 donor per cell type, triplicate wells per donor, duplicate qPCR reactions averaged per well; mean±SD; **p<0.01, ***p<0.001, ****p<0.0001; ND=not detected. **B and D**, Representative Alizarin red staining of target knockdown in hCtASMCs (**B**) and hVICs (**D**) at days 14-21 in NM or pro-calcifying medium (PM) culture. **E and F**, Quantification of solubilized Alizarin red stain in hCtASMCs (**E**) and hVICs (**F**) treated as in B and D for 14 and 21 days confirmed that knockdown of *PPP2CA*, *ADAM17*, *APP*, and *APC* significantly inhibited calcification in both cell types, while knockdown of *FGFR2* inhibited hCtASMC calcification and knockdown of *WNT5A* significantly altered calcification only in hVICs; n=3 hCtASMC donors and 3 hVIC donors, duplicate wells averaged per timepoint per donor; *p<0.05, **p<0.01, ***p<0.001. Grey bars indicate the minimum to maximum intensity range of the NM siSCR condition. Corresponds to Figure 7E-J.

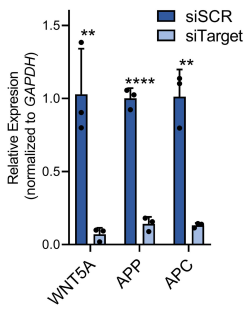
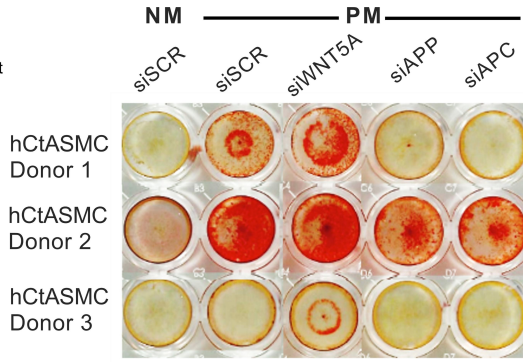
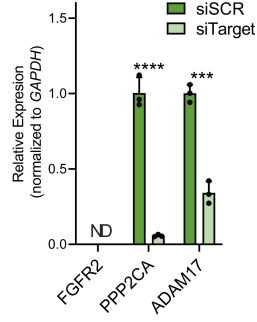
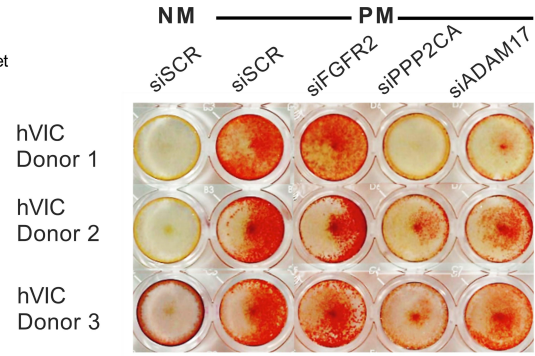
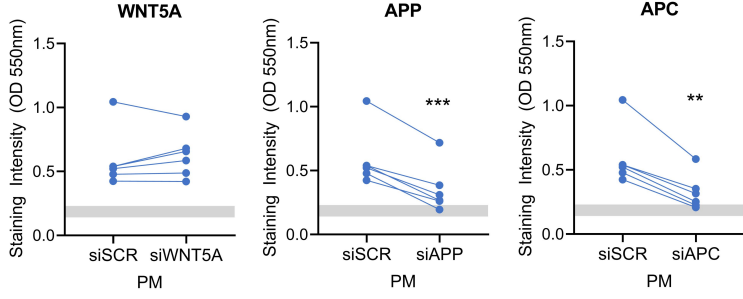
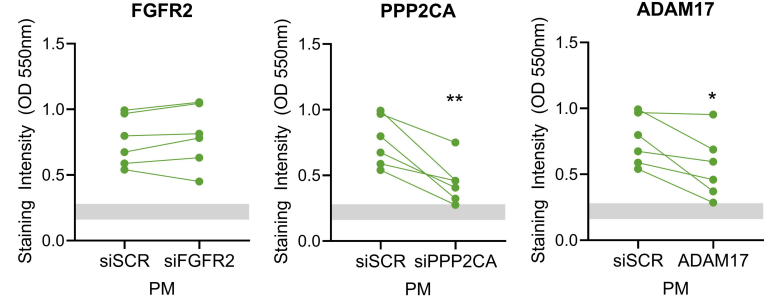
A**hCtASMC mRNA****B****hCtASMC Alizarin Red (calcification)****C****hVIC mRNA****D****hVIC Alizarin Red (calcification)****E****Alizarin Red****F****Alizarin Red**

Figure S25: Quantification of Baseline hCtASMC and hVIC Calcification. Quantification of solubilized Alizarin red stain in hCtASMCs and hVICs incubated with scrambled siRNA (siSCR) or siRNA targeting *WNT5A*, *APP*, *APC*, *FGFR2*, *PPP2CA*, and *ADAM17* (siWNT5A, siAPP, siAPC, siFGFR2, siPPP2CA, siADAM17) for 14 and 21 days in normal medium (NM) demonstrated little baseline calcification under normal culture conditions, without significant alterations between siSCR and target treatments; n=3 hCtASMC donors and 3 hVIC donors, duplicate wells averaged per timepoint per donor. Corresponds to Figure 7E-J and Figure S24.

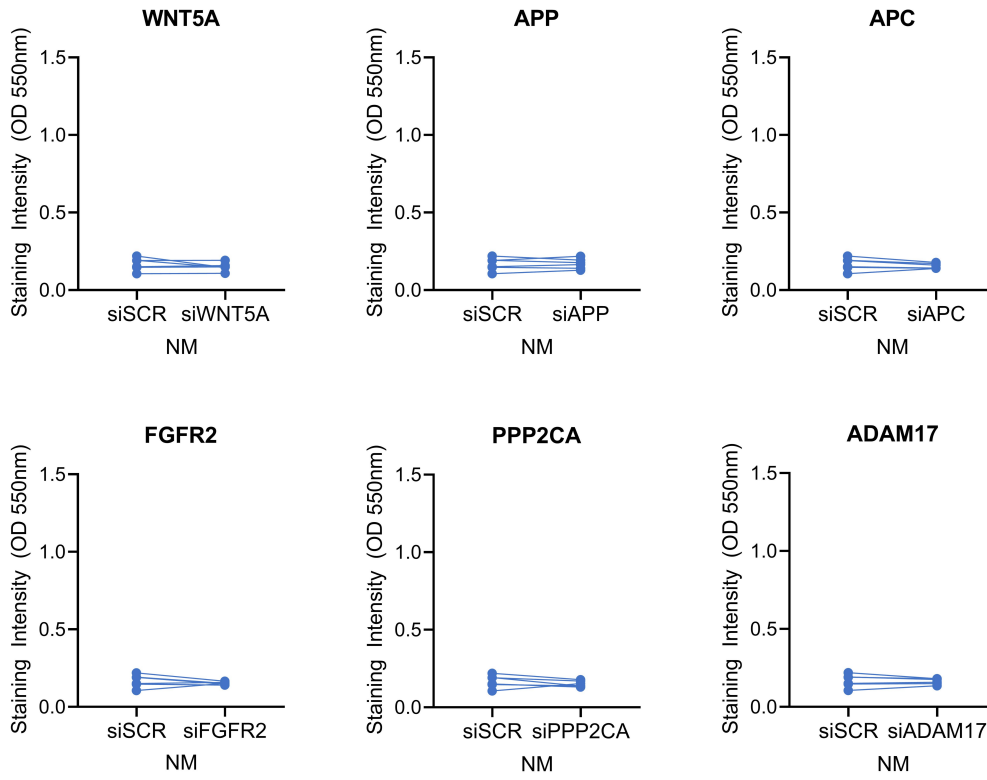
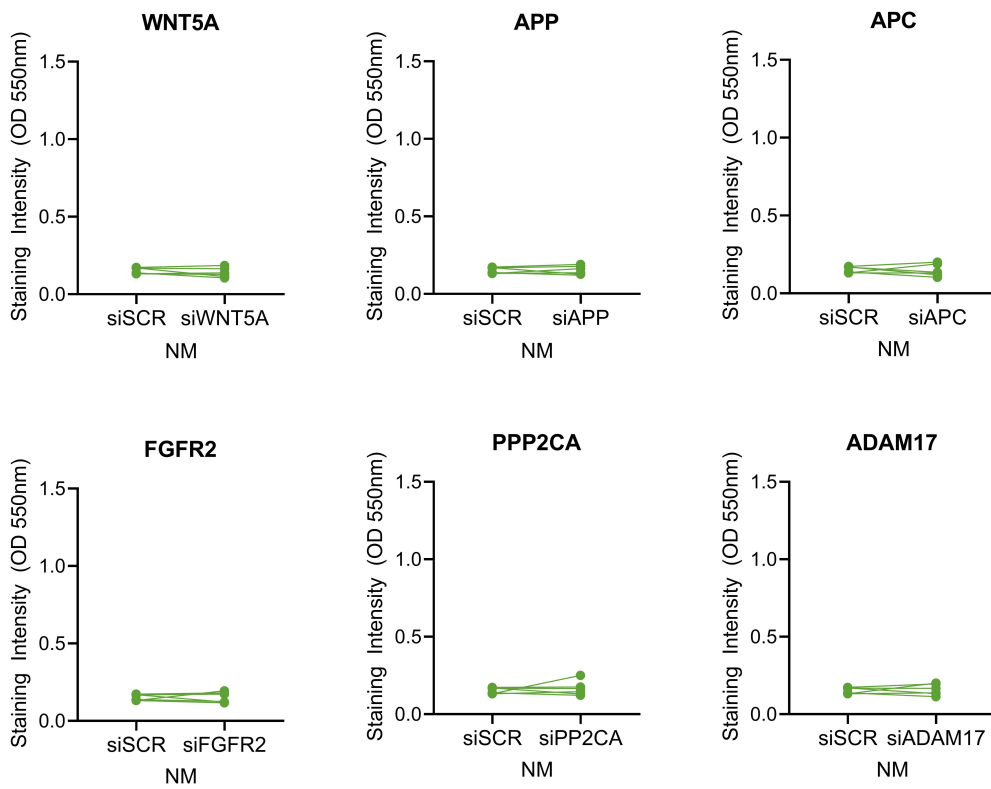
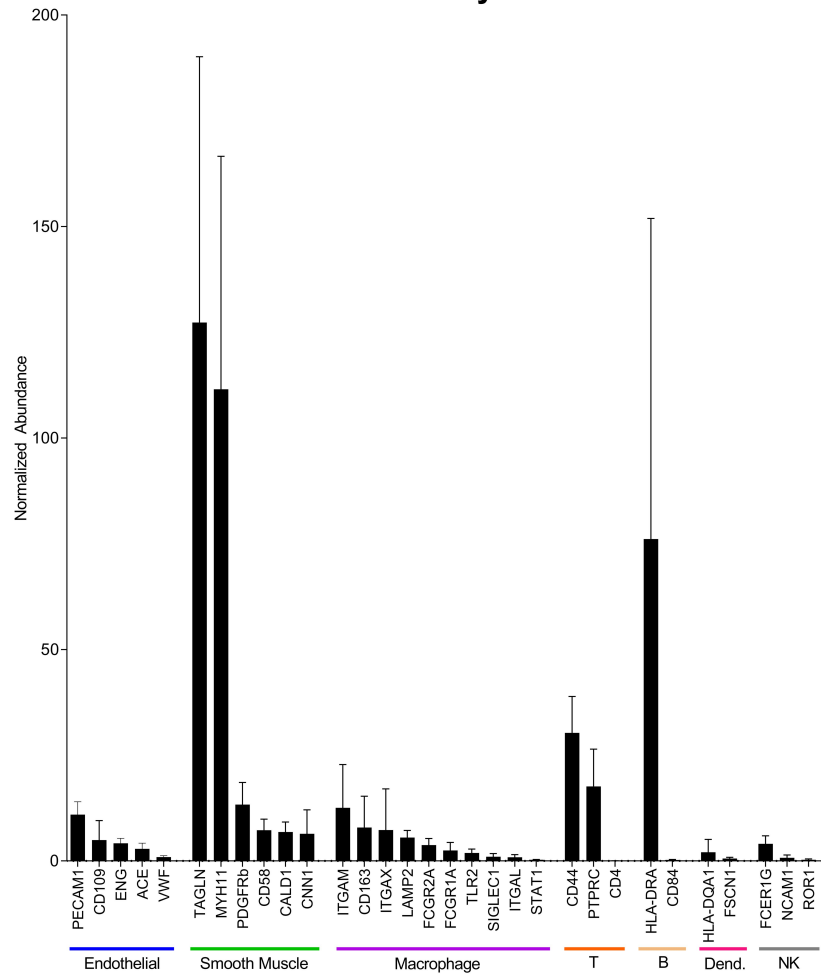
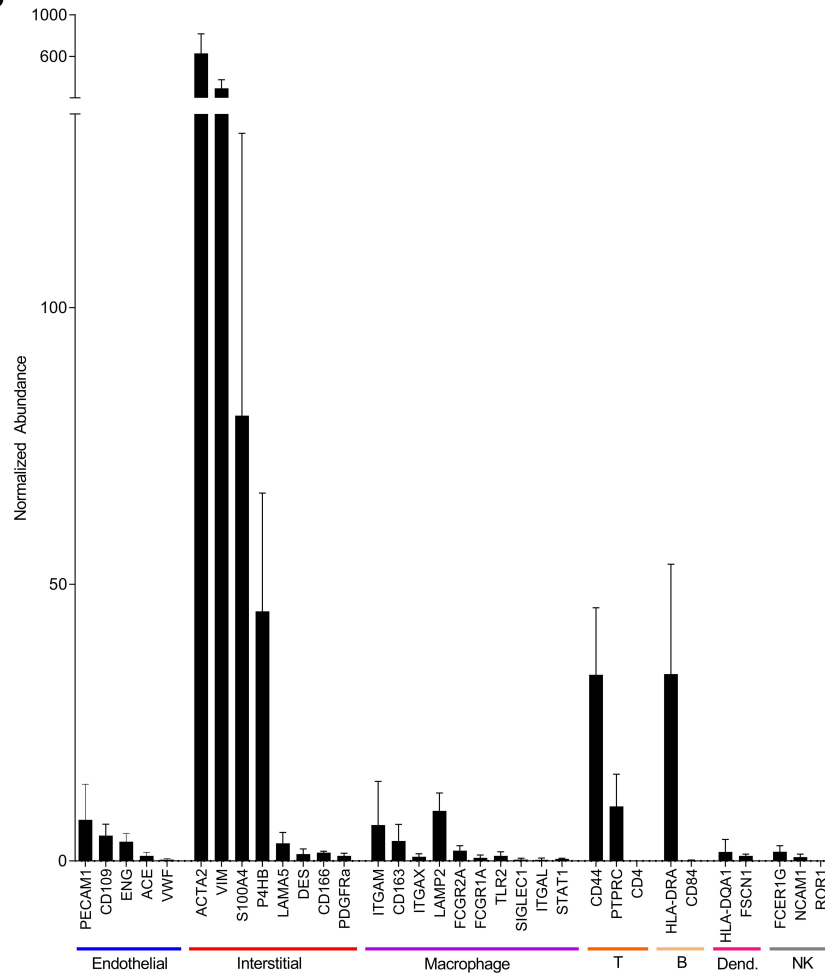
A**hCtASMC Alizarin Red****B****hVIC Alizarin Red**

Figure S26: Quantification of Cell Type Markers in Tissue EVs. Proteomics-derived normalized protein abundances of selected cell type-specific markers of endothelial cells, smooth muscle or valvular interstitial cells, macrophages, T cells (T), B cells (B), dendritic cells (Dend.), or natural killer cells (NK) in tissue EVs isolated by density gradient separation from intact carotid arteries (n=10 donors, **A**), and intact aortic valves (n=10, **B**). Mean \pm SD. Corresponds to Figure 4.

A**Carotid Artery EVs****B****Aortic Valve EVs**

Median Normalization Data Processing Script

```
import os
import re
import csv
import numpy
import sys
from tkinter import *
from tkinter import filedialog

def append_string(short_string, template, glue):
    """
    :param short_string:    short string to append the template
    :param template:       the template to be prolonged
    :param glue:           characters to be located between short and
template
    :return:                string type
    """
    if template == '':
        return short_string
    else:
        return template + glue + short_string

print("File path you want to process: ")
root = Tk()
file_path = filedialog.askopenfilename(initialdir = "~/`Syncplicity
Folders`/Label-free",title = "choose your file",filetypes = (("PD2.2
export","*.txt"),("all files","*.*)""))
root.withdraw()

# Get unique peptide threshold
min_uniq = 1
while True:
    input_num = input("\n\nMinimum the number of unique peptide (most
recommended number: 2, Q for quit): ")
    if (input_num.upper()=="Q"):
        print("Bye!")
        exit()
    elif (input_num.isdigit()):
        min_uniq = int(input_num)
        break
    else:
        print("{0} is not a number".format(input_num))

dict_gn2uni = {}
dict_uni2data = {}
list_colnames = []
```

```

flag_no_annotation = False
rows = csv.DictReader(open(file_path), delimiter='\t')
for row in rows:
    # Get protein information
    uniprot = row["Accession"]
    desc = row["Description"]
    try:
        gene_name = desc.split('GN=')[1].split()[0]
    except IndexError:
        gene_name = uniprot
    if gene_name not in dict_gn2uni:
        dict_gn2uni[gene_name] = {}
        dict_gn2uni[gene_name][uniprot] = {'psm': int(row["# PSMs"]),
"uniq_pep": int(row["# Unique Peptides"]), "aa": int(row["# AAs"])}

    # Get annotations
    try:
        dict_uni2data[uniprot] = {'desc': desc, 'bp':row["Biological
Process"], 'cc':row["Cellular Component"],
                                'mf':row["Molecular Function"],
'kegg':row["KEGG Pathways"]}
        flag_no_annotation = True
    except KeyError:
        dict_uni2data[uniprot] = {'desc': desc}
        flag_no_annotation = False

    # Get expression profile
    for colname in row:
        if re.match('Abundance', colname):
            if colname not in list_colnames:
                list_colnames.append(colname)
            try:
                auc = float(row[colname])
            except ValueError:
                auc = 0
            dict_uni2data[uniprot][colname] = auc

dict_col2values = {}
fp_out = open("filtered.xls", "w")
header =
"Gene_name\tUniProt\tDescription\t#_AA\t#_Unique_peptides\tPSM\tGO_BP\t
GO_CC\tGO_MF\tKEGG\t{0}\n".format("\t".join(list_colnames))
fp_out.write(header)
for gn in dict_gn2uni:
    aa = 0
    uq = 0
    psm = 0
    out_string = ""

```

```

for uniprot in dict_gn2uni[gn]:
    data = dict_uni2data[uniprot]
    uni_info = dict_gn2uni[gn][uniprot]
    flag = False
    if aa < uni_info["aa"]:
        flag = True
        aa = uni_info["aa"]
        uq = uni_info["uniq_pep"]
        psm = uni_info["psm"]
    elif aa == uni_info["aa"]:
        if uq < uni_info["uniq_pep"]:
            flag = True
            aa = uni_info["aa"]
            uq = uni_info["uniq_pep"]
            psm = uni_info["psm"]
        elif uq == uni_info["uniq_pep"]:
            if psm < uni_info["psm"]:
                flag = True
                aa = uni_info["aa"]
                uq = uni_info["uniq_pep"]
                psm = uni_info["psm"]
            else:
                flag = False
        else:
            flag = False
    else:
        flag = False

if flag:
    if flag_no_annotation:
        if data['kegg'] == "":
            kegg = "NA"
        else:
            kegg = data['kegg']
        if data['mf'] == "":
            mf = "NA"
        else:
            mf = data['mf']
        if data['cc'] == "":
            cc = "NA"
        else:
            cc = data['cc']
        if data['bp'] == "":
            bp = "NA"
        else:
            bp = data['bp']
    else:
        kegg = "NA"

```

```

        mf = "NA"
        cc = "NA"
        bp = "NA"
        if uni_info['uniq_pep'] < min_uniq:
            continue
        out_string =
"{0}\t{1}\t{2}\t{3}\t{4}\t{5}\t{6}\t{7}\t{8}\t{9}".format(
            gn, uniprot, data['desc'], str(uni_info['aa']),
str(uni_info['uniq_pep']), str(uni_info['psm']), bp, cc, mf, kegg)
        for colname in list_colnames:
            if colname not in dict_col2values:
                dict_col2values[colname] = []
            value = data[colname]
            if value != 0:
                dict_col2values[colname].append(value)
            out_string = append_string(str(value), out_string,
"\t")
        if out_string != "":
            fp_out.write(out_string+"\n")
fp_out.close()

fp_out = open("filtered_and_normalized.xls", "w")
fp_out.write(header)
rows = csv.DictReader(open("filtered.xls"), delimiter='\t')
for row in rows:
    out_string =
"{0}\t{1}\t{2}\t{3}\t{4}\t{5}\t{6}\t{7}\t{8}\t{9}".format(
row["Gene_name"], row["UniProt"], row["Description"], row["#_AA"], row["#_
Unique_peptides"],
    row["PSM"], row["GO_BP"], row["GO_CC"], row["GO_MF"], row["KEGG"])
    for colname in list_colnames:
        value =
float(row[colname])/numpy.median(dict_col2values[colname])
        out_string = append_string(str(value), out_string, "\t")
    fp_out.write(out_string+"\n")
fp_out.close()

fp_out = open("data_summary.xls", "w")
fp_out.write("Column name\tMedian intensity\t# of Proteins\n")
for colname in list_colnames:
    fp_out.write("{0}\t{1}\t{2}\n".format(colname,
numpy.median(dict_col2values[colname]),
numpy.count_nonzero(dict_col2values[colname])))
fp_out.close()

```